THE JOURNAL OF DERMATOLOGY

doi: 10.1111/1346-8138.12810

Journal of Dermatology 2015; **42**: 528–531

CONCISE COMMUNICATION

Serum vaspin levels: A possible correlation with digital ulcers in patients with systemic sclerosis

Shunsuke MIURA, Yoshihide ASANO, Ryosuke SAIGUSA, Takashi YAMASHITA, Takashi TANIGUCHI, Takehiro TAKAHASHI, Yohei ICHIMURA, Tetsuo TOYAMA, Zenshiro TAMAKI, Yayoi TADA, Makoto SUGAYA, Shinichi SATO, Takafumi KADONO

Department of Dermatology, University of Tokyo Graduate School of Medicine, Tokyo, Japan

ABSTRACT

Vaspin is an adipokine implicated in vascular inflammation and remodeling. We herein evaluated the clinical correlation of serum vaspin levels in systemic sclerosis (SSc). Consistent with previous reports, 12% of subjects exhibited serum vaspin levels over 10 ng/mL, likely due to genetic effects. Excluding these subjects, despite no difference between SSc and control subjects, serum vaspin levels were significantly decreased in SSc patients with digital ulcers compared with those without, suggesting the potential contribution of vaspin to digital ulcers of this disease.

Key words: digital ulcers, endothelial cells, systemic sclerosis, vascular smooth muscle cells, vaspin.

INTRODUCTION

Systemic sclerosis (SSc) is a multisystem autoimmune disease characterized by vasculopathy and tissue fibrosis with unknown etiology. Recently, adipokines have attracted much attention as a cytokine family contributing to the various pathological processes of SSc.

Vaspin is an adipokine expressed predominantly in visceral adipose tissue and plays important roles in metabolic syndrome and its relevant vascular complications. For example, serum vaspin levels correlate positively with hemoglobin A1c and negatively with insulin levels and Homeostasis Model of Assessment in type 2 diabetes mellitus (T2DM) patients. Furthermore, T2DM patients with microangiopathy have serum vaspin levels that are significantly lower than those without. Moreover, a potential protective impact of vaspin against atherosclerosis through anti-inflammatory and anti-apoptotic effects on vascular smooth muscle cells (vSMC) and endothelial cells (EC) has been disclosed *in vitro* and serum vaspin levels are significantly decreased in T2DM patients with carotid plaque compared with those without.[1] On the other hand, vaspin seems to be involved in autoimmune inflammatory diseases and fibrotic liver diseases. For instance, vaspin levels in sera and synovial fluid are elevated in rheumatoid arthritis patients,[2,3] while serum vaspin levels are decreased in Behçet's disease patients.[3] Also, there is a positive correlation between serum vaspin levels and angiogenesis intensity of portal tracts and lobules in chronic hepatitis C patients.[4] Thus, vaspin is likely to be involved in various pathological conditions other than glucose metabolism, especially vascular inflammation and remodeling, which are related to SSc vasculopathy. Therefore, we investigated the clinical correlation of serum vaspin levels in SSc patients.

METHODS

Patients

Serum samples, frozen at −80°C until assayed, were obtained from 67 SSc patients and 19 healthy individuals after getting informed consent and institutional approval (University of Tokyo Graduate School of Medicine). Patients who had been treated with corticosteroids or other immunosuppressants were excluded. No patient had diabetes. Patients were grouped by LeRoy's classification system: 36 patients with limited cutaneous SSc (lcSSc) and 31 with diffuse cutaneous SSc (dcSSc). All patients fulfilled the new classification criteria of SSc.[5] Patient information is summarized in Figure 1.

Measurement of serum vaspin levels

Specific enzyme-linked immunosorbent assay kits were used to measure serum vaspin levels (BioVendor Laboratory Medicine, Brno, Czech Republic). Briefly, 96-well polystyrene plates coated with anti-vaspin antibodies were incubated with threefold diluted serum at room temperature for 1 h. After washing the wells, biotin-labeled polyclonal anti-human vaspin antibody was added and incubated with the captured vaspin for 1 h. Then, the wells were washed and incubated at room temperature for 30 min with horseradish peroxidase-conjugated streptavidin. Next, the wells were washed again,

Correspondence: Yoshihide Asano, M.D., Ph.D., or Takafumi Kadono, M.D., Ph.D., Department of Dermatology, University of Tokyo Graduate School of Medicine, 7-3-1 Hongo, Bunkyo-ku, Tokyo 113-8655, Japan.
Email: yasano-tky@umin.ac.jp or kadono-der@h.u-tokyo.ac.jp
Received 2 December 2014; accepted 7 January 2015.

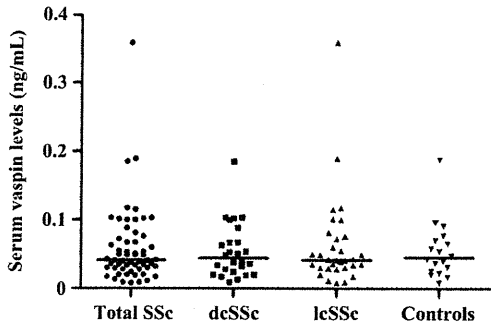

	Total SSc	dcSSc	lcSSc	Controls
Sex (male : female)	2 : 65	1 : 30	1 : 35	1 : 18
Age (years)	59 (48-69)	51 (46-63)	63.5 (54.5-72.5)	53 (45-67)
Disease duration (years)	6 (2-18)	5 (2-18)	6.5 (2-16.3)	
BMI (kg/m^2)	20.6 (18.6-22.9)	20.5 (18.6-22.4)	20.6 (18.6-23.0)	23.0 (20.1-24.1)
Vaspin (ng/mL)	0.125 (0.088-0.212)	0.134 (0.075-0.161)	0.125 (0.09-0.219)	0.137 (0.08-0.206)

Figure 1. Serum vaspin levels in systemic sclerosis (SSc) patients and healthy controls. Serum vaspin levels were determined by a specific enzyme-linked immunoassay in total SSc, diffuse cutaneous (dc)SSc, limited cutaneous (lc)SSc and healthy controls. Bars indicate the median value in each group. Statistical analysis was carried out with one-way ANOVA followed by Tukey's post-hoc test for multiple comparison. Patient information of each group is described below the graph. The values represent median with 25–75 percentiles in parenthesis. BMI, body mass index. In the graph and the calculation of median and 25–75 percentiles of serum vaspin levels, subjects with serum vaspin levels over 10 ng/ml were excluded.

tetramethyl-benzidine was added and incubated at room temperature for 10 min. Finally, H_2SO_4 was added to terminate the reaction and absorbance at 450 nm was measured. Serum vaspin levels were calculated using a standard curve.

Clinical assessment

Disease onset was defined as the first clinical event that was a clear manifestation of SSc other than Raynaud's phenomenon. The duration of disease was defined as the interval between the onset and the time of blood sampling. The details of assessment for organ involvement are described in the legend of Table 1 and a previous report.[6]

Statistical analysis

Statistical analysis was carried out with the Mann–Whitney *U*-test to compare the distributions of two unmatched groups, with one-way ANOVA followed by Tukey's post-hoc test for multiple comparison, with Fisher's exact probability test for the analysis of frequency, and with Spearman's rank correlation coefficient to evaluate the correlation with clinical data. Statistical significance was set at $P < 0.05$.

RESULTS

Serum vaspin levels in SSc

A fraction of the Japanese population, approximately 7%, exhibits 10-fold higher serum vaspin levels (>10 ng/mL) due to genetic effects.[7] Consistently, nine of 67 SSc patients (13%) and one of 19 healthy controls (5.3%) had serum vaspin levels higher than 10 ng/mL. The frequency was not statistically different between SSc and healthy subjects ($P = 0.45$) and we confirmed no clinical difference between SSc patients with serum vaspin levels over 10 ng/mL and the others (data not shown). Because these individuals appeared to have serum vaspin levels over 10 ng/mL genetically, we excluded them in the following analyses.

Serum vaspin levels correlated with neither body mass index nor serum low-density lipoprotein levels in SSc patients ($r = 0.21$ [$P = 0.12$] and $r = -0.03$ [$P = 0.81$], respectively) and were comparable among total SSc, dcSSc, lcSSc and healthy controls (Fig. 1). Furthermore, serum vaspin levels correlated with none of modified Rodnan Skin Score, vital capacity and diffusing capacity of the lung for carbon monoxide in SSc patients (data not shown). Collectively, vaspin appears not to contribute to fibrotic and metabolic conditions in SSc patients.

Clinical correlation of serum vaspin levels in SSc

We next compared serum vaspin levels between SSc patients with each clinical symptom and the others (Table 1). The presence of cutaneous vascular involvement, including Raynaud's phenomenon, nailfold bleeding and telangiectasia, did not affect serum vaspin levels. As for vascular organ involvement relevant to proliferative obliterative vasculopathy, the presence of digital ulcers (DU) was associated with a significant decrease of serum vaspin levels (Fig. 2), while pulmonary vascular involvement characterized by elevated right ventricular systolic pressure did not alter serum vaspin levels. Regarding scleroderma renal crisis (SRC), serum vaspin levels were comparable between patients with this complication and those without, although it was not convincing due to the small number of cases with SRC. The other visceral involvement relevant to microangiopathy and fibrosis, including interstitial lung disease, esophagus dysfunction and heart involvement, did not cause a significant change in serum vaspin levels. Finally, we confirmed no correlation of serum vaspin levels with C-reactive protein and erythrocyte sedimentation rate, indicating little role of vaspin in the inflammatory process of SSc. Collectively, vaspin may be involved in the development of DU in SSc patients.

DISCUSSION

Similar to other adipokines, vaspin affects vascular homeostasis through anti-inflammatory and anti-apoptotic effects on vSMC and EC. In vSMC, tumor necrosis factor (TNF)-α upregulates intercellular adhesion molecule-1 (ICAM-1) through reactive oxygen species (ROS) generation and platelet-derived growth factor-BB induces migration. Vaspin inhibits these processes,

Table 1. Associations of serum vaspin levels with clinical features in SSc patients

	Serum vaspin levels (ng/mL)		
Clinical symptoms	Patients with symptoms	Patients without symptoms	*P*
Raynaud's phenomenon	0.042 (0.028–0.072) (*n* = 55)	0.035 (0.032–0.076) (*n* = 3)	0.52
Nail-fold bleeding	0.046 (0.034–0.077) (*n* = 42)	0.033 (0.021–0.054) (*n* = 16)	0.97
Telangiectasia	0.049 (0.027–0.077) (*n* = 30)	0.038 (0.030–0.054) (*n* = 23)	0.99
Digital ulcers	0.030 (0.020–0.039) (*n* = 15)	0.049 (0.034–0.088) (*n* = 43)	0.0069*
Esophageal dysfunction	0.041 (0.028–0.081) (*n* = 43)	0.042 (0.030–0.063) (*n* = 15)	0.27
Heart involvement	0.058 (0.018–0.111) (*n* = 8)	0.041 (0.030–0.068) (*n* = 50)	0.56
Interstitial lung disease	0.042 (0.028–0.088) (*n* = 31)	0.041 (0.029–0.060) (*n* = 27)	0.88
Elevated RVSP	0.035 (0.017–0.067) (*n* = 11)	0.042 (0.030–0.076) (*n* = 47)	0.75
Scleroderma renal crisis	0.078 (0.055–0.101) (*n* = 2)	0.041 (0.028–0.071) (*n* = 56)	0.56

Interstitial lung disease was defined as bibasilar interstitial fibrosis on chest radiographs or alveolitis on high-resolution computer tomography. Elevated right ventricular systolic pressure (RVSP) was defined as ≥35 mmHg on echocardiogram. Scleroderma renal crisis was defined as malignant hypertension and/or rapidly progressive renal failure. Statistical analysis was carried out with Fisher's exact probability test. *$P < 0.05$. Median (25–75 percentiles) is shown for each group.

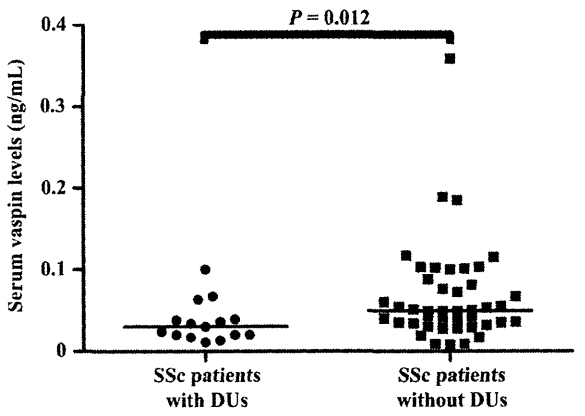

Figure 2. Serum vaspin levels in systemic sclerosis (SSc) patients with or without digital ulcers. Serum vaspin levels were determined by a specific enzyme-linked immunoassay. The horizontal bars indicate the median value in each group. Statistical analysis was carried out with the Mann–Whitney *U*-test. DUs, digital ulcers.

resulting in the suppression of vascular inflammation and atherosclerosis. Under a diabetic condition, vaspin suppresses high-glucose-induced proliferation and chemokinesis of vSMC and apoptosis of EC via the inhibition of ROS generation. Vaspin also protects EC from TNF-α and interleukin-1-induced inflammation and from free fatty acid-induced apoptosis.[1] Consistently, diabetic rats infected with adenovirus expressing vaspin are resistant to intimal proliferation of balloon-injured carotid arteries.[8] On the other hand, in chronic hepatitis C, vaspin seems to be involved in the pathological angiogenesis.[4] Thus, vaspin is deeply involved in the pathological vascular remodeling and angiogenesis.

Recent studies have revealed the potential contribution of adipokines to SSc vasculopathy. For example, elevated serum resistin levels and decreased serum retinol binding protein-4 levels are associated with pulmonary arterial hypertension (PAH)[9,10] and increased serum apelin levels are linked to the prevalence of severe vascular involvement related to proliferative obliterative vasculopathy.[11] In the present study, the decrease in serum vaspin levels was linked to DU in SSc patients. Given that proliferative obliterative vasculopathy underlying DU has a complicated pathological process including EC apoptosis, vSMC proliferation and their phenotypical changes, a decrease of vaspin concentration in peripheral circulation may contribute to the development of SSc-associated DU in concert with various factors including other adipokines.

Recently, anti-ICAM-1 antibody with an agonistic effect inducing ROS generation and subsequent apoptosis of EC was identified in SSc.[12] Given that ROS induces ICAM-1 expression in vSMC,[13] anti-ICAM-1 antibody augments vascular inflammatory response in SSc. Vaspin has a potent anti-inflammatory effect on vasculature by preventing ROS production, but this inhibitory system is likely to be less functional in SSc patients with DU due to a decrease of serum vaspin levels. SSc vasculopathy is a gradual, but progressive, pathological process along with disease duration and finally results in severe vascular complications such as DU, PAH and SRC. Behind these, there is a highly orchestrated pathological process in which some members of adipokines are involved. It is already known that a certain set of adipokines are mutually regulated by each other and that vaspin suppresses the expression of TNF-α, resistin and leptin.[1] Because serum levels of TNF-α, resistin and leptin are increased in SSc patients,[14] a hierarchical regulation network of the adipokine production is retained even in the pathological condition of SSc. Given that the elevated serum levels of resistin, which enhances endothelin-1 production in EC,[15] are associated with SSc-PAH,[9] a certain set of adipokines may accelerate the development of SSc vasculopathy as a result of their accumulative effects on vasculature.

The present study further supports the idea that adipokines are a new member of cytokines involved in the pathological process of SSc.

ACKNOWLEDGMENTS: This work was supported by a grant for Research on Intractable Diseases from the Ministry of Health, Labor and Welfare of Japan.

CONFLICT OF INTEREST: The authors have declared no conflicts of interest.

REFERENCES

1 Heiker JT. Vaspin (serpinA12) in obesity, insulin resistance, and inflammation. *J Pept Sci* 2014; **20**: 299–306.
2 Senolt L, Polanská M, Filková M *et al.* Vaspin and omentin: new adipokines differentially regulated at the site of inflammation in rheumatoid arthritis. *Ann Rheum Dis* 2010; **69**: 1410–1411.
3 Ozgen M, Koca SS, Dagli N, Balin M, Ustundag B, Isik A. Serum adiponectin and vaspin levels in rheumatoid arthritis. *Arch Med Res* 2010; **41**: 457–463.
4 Kukla M, Berdowska A, Gabriel A *et al.* Association between hepatic angiogenesis and serum adipokine profile in non-obese chronic hepatitis C patients. *Pol J Pathol* 2011; **62**: 218–228.
5 van den Hoogen F, Khanna D, Fransen J *et al.* 2013 classification criteria for systemic sclerosis: an American College of Rheumatology/European League against Rheumatism collaborative initiative. *Arthritis Rheum* 2013; **65**: 2737–2747.
6 Noda S, Asano Y, Aozasa N *et al.* Clinical significance of serum soluble Tie1 levels in patients with systemic sclerosis. *Arch Dermatol Res* 2013; **305**: 325–331.
7 Teshigawara S, Wada J, Hida K *et al.* Serum vaspin concentrations are closely related to insulin resistance, and rs77060950 at SERPINA12 genetically defines distinct group with higher serum levels in Japanese population. *J Clin Endocrinol Metab* 2012; **97**: E1202–E1207.
8 Nakatsuka A, Wada J, Iseda I *et al.* Visceral adipose tissue-derived serine proteinase inhibitor inhibits apoptosis of endothelial cells as a ligand for the cell-surface GRP78/voltage-dependent anion channel complex. *Circ Res* 2013; **112**: 771–780.
9 Masui Y, Asano Y, Akamata K *et al.* Serum resistin levels: a possible correlation with pulmonary vascular involvement in patients with systemic sclerosis. *Rheumatol Int* 2014; **34**: 1165–1170.
10 Toyama T, Asano Y, Takahashi T *et al.* Clinical significance of serum retinol binding protein-4 levels in patients with systemic sclerosis. *J Eur Acad Dermatol Venereol* 2013; **27**: 337–344.
11 Aozasa N, Asano Y, Akamata K *et al.* Serum apelin levels: clinical association with vascular involvements in patients with systemic sclerosis. *J Eur Acad Dermatol Venereol* 2013; **27**: 37–42.
12 Wolf SI, Howat S, Abraham DJ, Pearson JD, Lawson C. Agonistic anti-ICAM-1 antibodies in scleroderma: activation of endothelial pro-inflammatory cascades. *Vascul Pharmacol* 2013; **59**: 19–26.
13 Phalitakul S, Okada M, Hara Y, Yamawaki H. Vaspin prevents TNF-α-induced intracellular adhesion molecule-1 via inhibiting reactive oxygen species-dependent NF-κB and PKCθ activation in cultured rat vascular smooth muscle cells. *Pharmacol Res* 2011; **64**: 493–500.
14 Pehlivan Y, Onat AM, Ceylan N *et al.* Serum leptin, resistin and TNF-α levels in patients with systemic sclerosis: the role of adipokines in scleroderma. *Int J Rheum Dis* 2012; **15**: 374–379.
15 Verma S, Li SH, Wang CH *et al.* Resistin promotes endothelial cell activation: further evidence of adipokine-endothelial interaction. *Circulation* 2003; **108**: 736–740.

ARTHRITIS & RHEUMATOLOGY
Vol. 67, No. 5, May 2015, pp 1335–1344
DOI 10.1002/art.39062

Endothelin Receptor Blockade Ameliorates Vascular Fragility in Endothelial Cell–Specific Fli-1–Knockout Mice by Increasing Fli-1 DNA Binding Ability

Kaname Akamata,[1] Yoshihide Asano,[1] Takashi Yamashita,[1] Shinji Noda,[1] Takashi Taniguchi,[1] Takehiro Takahashi,[1] Yohei Ichimura,[1] Tetsuo Toyama,[1] Maria Trojanowska,[2] and Shinichi Sato[1]

Objective. **It is generally accepted that blockade of endothelin receptors has potentially beneficial effects on vasculopathy associated with systemic sclerosis (SSc). The aim of this study was to clarify the molecular mechanism underlying these effects using endothelial cell–specific Fli-1–knockout (Fli-1 ECKO) mice, an animal model of SSc vasculopathy.**

Methods. **Levels of messenger RNA for target genes and the expression and phosphorylation levels of target proteins were determined in human and murine dermal microvascular endothelial cells by real-time quantitative reverse transcription–polymerase chain reaction and immunoblotting, respectively. The binding of Fli-1 to the target gene promoters was evaluated using chromatin immunoprecipitation. Expression levels of Fli-1 and α-smooth muscle actin in murine skin were evaluated using immunohistochemistry. Vascular structure and permeability were evaluated in mice injected with fluorescein isothiocyanate–dextran and Evans blue dye, respectively.**

Results. **In human dermal microvascular endothelial cells, endothelin 1 induced phosphorylation of Fli-1 at Thr^{312} through the sequential activation of c-Abl and protein kinase Cδ, leading to a decrease in Fli-1 protein levels as well as a decrease in binding of Fli-1 to the target gene promoters, whereas bosentan treatment reversed those effects. In Fli-1 ECKO mice, 4 weeks of treatment with bosentan increased endothelial Fli-1 expression, resulting in vascular stabilization and the restoration of impaired leaky vessels.**

Conclusion. **The vascular fragility of Fli-1 ECKO mice was improved by bosentan through the normalization of Fli-1 protein levels and activity in endothelial cells, which may explain, in part, the mechanism underlying the beneficial effects of endothelin receptor blockade on SSc vasculopathy.**

Systemic sclerosis (SSc) is a multisystem connective tissue disease characterized by immunologic abnormalities, vasculopathy, and resultant fibrosis of the skin and certain internal organs (1). Although the pathogenesis of SSc currently remains elusive, studies have demonstrated that bosentan, a dual endothelin receptor antagonist, prevents the development of new digital ulcers in SSc patients (2,3), suggesting a critical role of endothelin in the mechanism underlying SSc vasculopathy. The effect of bosentan on nailfold capillary changes is still up for debate, but previous studies have revealed that bosentan, alone or together with iloprost, fosters microvascular de-remodeling in nailfold capillaries (4–6), where morphologic changes mostly progress in parallel with disease duration and are refractory to canonical treatments such as prostanoids (5,7). These observations suggest that endothelin receptor blockade potentially has a disease-modifying impact on SSc vasculopathy.

Supported by the Ministry of Health, Labor, and Welfare of Japan (grants to Drs. Asano and Sato), the Japan Intractable Diseases Research Foundation, a Rohto Dermatology Prize, the Japanese Society for Investigative Dermatology Fellowship Shiseido Award, the Mochida Memorial Foundation for Medical and Pharmaceutical Research, and an Actelion Academia Award (to Dr. Asano). Dr. Trojanowska's work was supported by the NIH (grant AR-042334).

[1]Kaname Akamata, MD, PhD, Yoshihide Asano, MD, PhD, Takashi Yamashita, MD, Shinji Noda, MD, PhD, Takashi Taniguchi, MD, Takehiro Takahashi, MD, Yohei Ichimura, MD, Tetsuo Toyama, MD, Shinichi Sato, MD, PhD: University of Tokyo Graduate School of Medicine, Tokyo, Japan; [2]Maria Trojanowska, PhD: Boston University School of Medicine, Boston, Massachusetts.

Dr. Asano has received honoraria (less than $10,000) as well as research funding from Actelion.

Address correspondence to Yoshihide Asano, MD, PhD, Department of Dermatology, University of Tokyo Graduate School of Medicine, 7-3-1 Hongo, Bunkyo-ku, Tokyo 113-8655, Japan. E-mail: yasano-tky@umin.ac.jp.

Submitted for publication April 15, 2014; accepted in revised form February 3, 2015.

Fli-1 is a member of the Ets family of transcription factors, which have been implicated in the development of fibrosis and vasculopathy associated with SSc. In dermal fibroblasts, Fli-1 functions as a potent repressor of the *COL1A1* and *COL1A2* genes (8–10), and its deficiency acts to coordinately modulate the expression of fibrosis-related genes toward the establishment of a profibrotic phenotype (11–13). Importantly, the expression of the *Fli1* gene is markedly decreased in lesional SSc skin and SSc dermal fibroblasts, at least partly as a result of epigenetic suppression at the transcription level (14). Fli-1 protein levels are also notably decreased in dermal microvascular endothelial cells of lesional SSc skin as compared with those of normal skin (15). Furthermore, endothelial cell–specific Fli-1–knockout (Fli-1 ECKO) mice exhibit the histologic and functional abnormalities characteristic of SSc vasculopathy, such as distortion of arterioles with thickened and occluded vascular walls and increased permeability of capillaries (16). These previous data suggest that Fli-1 down-regulation contributes to the establishment of an SSc phenotype in dermal fibroblasts and dermal microvascular endothelial cells and that the reversal of Fli-1 expression is a potential therapeutic strategy for SSc.

In a recent study we showed that bosentan reverses the profibrotic phenotype of SSc dermal fibroblasts by increasing the DNA binding ability and the expression levels of Fli-1 (17). Given that SSc vasculopathy at least partly results from endothelial Fli-1 deficiency (12,13,16,18), we reasoned that the effect of bosentan on digital ulcers and nailfold capillary changes in SSc may involve the normalization of Fli-1 expression levels in endothelial cells. To assess this hypothesis, we investigated the impact of endothelin 1 (ET-1) and bosentan on the behavior of Fli-1 in endothelial cells and the effect of bosentan on vascular abnormalities in Fli-1 ECKO mice, an animal model of SSc vasculopathy.

MATERIALS AND METHODS

Reagents. Anti–Fli-1 antibodies for immunoblotting and anti–protein kinase Cδ (anti-PKCδ) antibodies were purchased from Santa Cruz Biotechnology. Anti–Fli-1 antibodies for immunohistochemistry were obtained from BD Biosciences. Antibodies against c-Abl and phospho–c-Abl (Tyr^{245}) were purchased from Cell Signaling Technology. Antibodies to β-actin were from Sigma-Aldrich. Polyclonal rabbit anti–phospho–Fli-1 (Thr^{312})–specific antibodies were generated as described previously (9). Bosentan was a gift from Actelion Pharmaceuticals.

Generation of Fli-1 ECKO mice. $Fli\text{-}1^{flx/flx}$ mice were generated as described previously (16). Mice expressing Cre recombinase under the control of the endothelium-specific tyrosine protein kinase receptor 2 promoter were purchased from The Jackson Laboratory and crossed with $Fli\text{-}1^{flx/flx}$ mice. Cre-mediated recombination of the flox allele in endothelial cells from different individual mice varied between 50% and 80% (16). All animal studies and procedures were approved by the Committee on Animal Experimentation of the University of Tokyo Graduate School of Medicine.

Cell culture. Human dermal microvascular endothelial cells (HDMECs) were purchased from Takara Bio. Murine dermal microvascular endothelial cells (MDMECs) were isolated from wild-type (WT) and Fli-1 ECKO mice. Briefly, newborn WT and Fli-1 ECKO mice (0–72 hours old) were killed by decapitation, rinsed in 70% ethanol, and the skin was removed. Excised mouse skin was placed in culture dishes dermis side down, with Dulbecco's modified Eagle's medium (DMEM) plus 3.5% Dispase (Sigma-Aldrich), and incubated at 4°C overnight. The dermis was separated from the epidermis, placed in DMEM plus 0.05% type I collagenase (Invitrogen), and incubated at 37°C for 1 hour. The cell suspension was filtered, centrifuged, stained with anti-CD31 microbeads (Miltenyi Biotec), and isolated using magnetic cell sorting. Isolation efficiency of MDMECs was decreased in Fli-1 ECKO mice as compared with WT mice, at least partially because of the decreased expression of CD31 on Fli-1–deficient mouse MDMECs as compared with WT mouse MDMECs (16). Endothelial cells were cultured on collagen-coated tissue culture plates in endothelial cell basal medium 2 (Cambrex) supplemented with endothelial cell growth media 2 SingleQuots (human vascular endothelial growth factor, epidermal growth factor, basic fibroblast growth factor, insulin-like growth factor 1, ascorbic acid, gentamicin, and heparin; Cambrex) and 5% heat-inactivated fetal bovine serum.

Cultured cells were assessed for a cobblestone appearance and specific staining for VE-cadherin and platelet endothelial cell adhesion molecule 1 (PECAM-1). Experiments were conducted with HDMECs and MDMECs at passages 1–3, in which a cobblestone appearance was maintained. Using a trypan blue exclusion test, we confirmed that ET-1 and bosentan at the concentrations used in this study did not affect the viability of HDMECs and/or MDMECs (data not shown).

Immunoblotting. Cells were grown to subconfluence and serum-starved when treated with the indicated reagents. Whole cell lysates and nuclear extracts were prepared as described previously (19,20). Samples were subjected to sodium dodecyl sulfate–polyacrylamide gel electrophoresis and immunoblotting with the indicated primary antibodies. Bands were detected using enhanced chemiluminescence techniques (Thermo Scientific).

RNA isolation and real-time quantitative reverse transcription–polymerase chain reaction (qRT-PCR). Total RNA was isolated from cultured endothelial cells with RNeasy spin columns (Qiagen). One microgram of total RNA from each sample was reverse transcribed into complementary DNA using the iScript cDNA Synthesis kit (Bio-Rad). Real-time qRT-PCR was performed using Fast SYBR Green PCR Master Mix (Applied Biosystems) on an ABI Prism 7000 (Applied Biosystems) in triplicate. The sequences of primers for Fli-1 and 18S ribosomal RNA (rRNA) were as follows: for human Fli-1, forward 5′-GGATGGCAAGGAACTGTGTAA-3′ and reverse 5′-GGTTGTATAGGCCAGCAG-3′; for mouse Fli-1,

forward 5′-ACTTGGCCAAATGGACGGGACTAT-3′ and reverse 5′-CCCGTAGTCAGGACTCCCG-3′; for human 18S rRNA, forward 5′-CGCCGCTAGAGGTGAAATTC-3′ and reverse 5′-TTGGCAAATGCTTTCGCTC-3′; and for mouse 18S rRNA, forward 5′-CGCCGCTAGAGGTGAAA TTC-3′ and reverse 5′-TTGGCAAATGCTTTCGCTC-3′. The $\Delta\Delta C_t$ method was used to compare target gene and housekeeping gene (18S rRNA) messenger RNA (mRNA) expression.

Chromatin immunoprecipitation (ChIP) assay. ChIP assay was performed using an EpiQuik ChIP kit (Epigentek). Briefly, cells were treated with 1% formaldehyde for 10 minutes. The crosslinked chromatin was then prepared and sonicated to an average size of 300–500 bp. The DNA fragments were immunoprecipitated with anti–Fli-1 antibody at 4°C. As a negative control, normal rabbit IgG was used. After reversal of crosslinking, the immunoprecipitated chromatin was quantified by qRT-PCR. Primer sequences for the promoters of murine target genes, including *Cdh5*, *Pecam1*, *Pdgfb*, and *Mmp9*, have been described previously (16). Primer sequences for the promoters of human target genes were as follows: for VE-cadherin/F-1493, 5′-ACAAAGGGAATTGGCAGATG-3′ and for VE-cadherin/R-1319, 5′-AGTGCTCTGTCCCCTGTGTT-3′; for PECAM-1/F-1039, 5′-GGCCCCAAAGGTCAATCTTA-3′ and for PECAM-1/R-820, 5′-GGGCAACAGAGTGAGACTCC-3′; for platelet-derived growth factor β (PDGFβ)/F-1371, 5′-GCTGGGACTACAGGAGCTTG-3′ and for PDGFβ/R-1216, 5′-CATCACCTTGGTCCAAATCC-3′; for matrix metalloproteinase 9 (MMP-9)/F-353, 5′-CTGGAGGCTTTCAGACCAAG-3′ and for MMP-9/R-150, 5′-AAGGGCTTACACCA CCTCCT-3′. Using electrophoresis, we confirmed the presence of 175 bp, 220 bp, 156 bp, 204 bp, 183 bp, 246 bp, 171 bp, and 204 bp amplicons for the promoters of the *CDH5*, *PECAM1*, *PDGFB*, *MMP9*, *Cdh5*, *Pecam1*, *Pdgfb*, and *Mmp9* genes, respectively. No nonspecific amplification was detected in these experiments.

Administration of bosentan to mice. Isoflurane-anesthetized mice (8 weeks old) were infused with bosentan (sodium salt; 20 mg/kg) in 200 μl of 0.9% saline intraperitoneally for 28 days continuously.

Immunohistochemistry. Immunohistochemistry analysis with a Vectastain ABC kit (Vector) was performed on formalin-fixed, paraffin-embedded tissue sections using antibodies against Fli-1 and α-smooth muscle actin (α-SMA) according to the manufacturer's instructions.

Vascular permeability assay. Evans blue dye (0.5%) in 200 μl of 0.9% saline was injected into the tail vein and animals were killed after 30 minutes. Intravascular Evans blue dye was removed by flushing the systemic vasculature with 30 ml of saline through a cannula placed in the aorta. The presence of vascular leakage was macroscopically evaluated in the skin.

Visualization of the dermal vascular structure by fluorescein isothiocyanate (FITC)–conjugated dextran injection. Mice were anesthetized, and 200 μl of FITC-conjugated dextran (2,000 kd [20 mg/ml in phosphate buffered saline]) was injected into the tail vein. After 5 minutes, mice were killed, and a full-thickness specimen of back skin (4 × 2 cm) was prepared. The skin specimen was placed directly on the slide (epidermis side up), and the structure of vascular network in the skin was visualized by fluorescence microscopy.

Statistical analysis. Statistical analysis was performed using one-way analysis of variance (ANOVA) followed by Tukey's post hoc test for multiple comparisons and Mann-Whitney U test for 2-group comparisons. A paired *t*-test was used for the comparison of normally distributed paired data. *P* values less than 0.05 were considered significant.

RESULTS

ET-1 regulates the transcriptional activity of Fli-1 in HDMECs. Since ET-1 regulates the transcriptional activity of Fli-1 in dermal fibroblasts (17), we initially investigated whether it affects the transcriptional activity of Fli-1 in HDMECs. Our previous studies have demonstrated that transcriptional activity of Fli-1 is tightly regulated by the phosphorylation/acetylation cascade triggered by the PKCδ-dependent phosphorylation of Fli-1 at Thr^{312} (9). Phosphorylated Fli-1 is subsequently acetylated by p300/CREB binding protein–associated factor at Lys^{380}, resulting in a loss of DNA binding ability and subsequent degradation (8). Since the phosphorylation of Fli-1 at Thr^{312} is a critical step in the regulation of Fli-1 transcriptional activity, we examined the effect of ET-1 on the phosphorylation levels of Fli-1 at Thr^{312}.

As shown in Figure 1A, consistent with our hypothesis, after 24 hours of ET-1 stimulation levels of Fli-1 phosphorylation at Thr^{312} were increased, while its total protein levels were decreased, in a dose-dependent manner (the mean ± SEM ratio of phospho–Fli-1 to total Fli-1 as compared with baseline was 2.76 ± 0.43, 9.05 ± 1.07, and 7.85 ± 1.26 with 50 n*M*, 100 n*M*, and 200 n*M* of ET-1, respectively; $P = 0.0004$ by one-way ANOVA, $P < 0.05$ for baseline versus 100 n*M* or 200 n*M* of ET-1 by Tukey's post hoc test). In contrast, ET-1 did not alter levels of mRNA for the *Fli1* gene under the same conditions (the mean ± SEM relative expression level of Fli-1 mRNA as compared with baseline was 0.96 ± 0.10, 0.90 ± 0.06, and 1.00 ± 0.17 with 50 n*M*, 100 n*M*, and 200 n*M* of ET-1, respectively; $P = 0.88$ by one-way ANOVA) (Figure 1B). These results suggest that ET-1 induces Fli-1 phosphorylation at Thr^{312}, leading to the decrease in Fli-1 protein levels through degradation, which is consistent with the previous observation in dermal fibroblasts (17). Since ET-1 at 200 n*M* did not affect the viability of HDMECs evaluated by trypan blue exclusion test (data not shown), we used 200 n*M* of ET-1 in the subsequent experiments.

To further investigate whether ET-1 decreases binding of Fli-1 to the target gene promoters, we used ChIP analysis. Since Fli-1 binds to the promoters of the *CDH5*, *PECAM1*, *PDGFB*, and *MMP9* genes and directly modulates their expression (16), we assessed the binding of Fli-1 to the promoter region of these

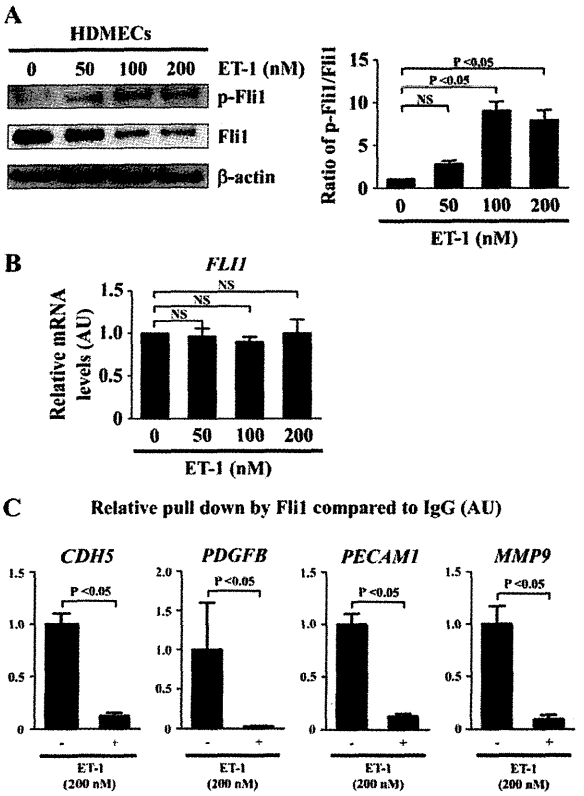

Figure 1. Effect of endothelin 1 (ET-1) on Fli-1 expression and function in human dermal microvascular endothelial cells (HDMECs). **A,** HDMECs were treated for 24 hours with ET-1 at the indicated concentrations, and the expression and phosphorylation levels of Fli-1 were determined by immunoblotting with whole cell lysates (β-actin was used as a control for equal loading). The fold change in the ratio of phospho–Fli-1 to total Fli-1 (quantified by densitometry) was determined. **B,** Levels of mRNA for Fli-1 after the same treatment as described in **A** were evaluated by quantitative reverse transcription–polymerase chain reaction (qRT-PCR). **C,** HDMECs were treated with ET-1 (200 n*M*) or vehicle for 2 hours and analyzed by chromatin immunoprecipitation. The binding of Fli-1 to the target gene promoters (*CDH5*, *PDGFB*, *PECAM1*, and *MMP9*) in response to ET-1 as compared to unstimulated controls (set at 1) was quantified by qRT-PCR. Values are the mean ± SEM (n = 3 mice per group). NS = not significant.

genes. As shown in Figure 1C, ET-1 decreased the binding of Fli-1 to the target gene promoters at 2 hours (the mean ± SEM relative pulldown by Fli-1 compared to IgG was 1.00 ± 0.11 at baseline versus 0.12 ± 0.03 after ET-1 stimulation, 1.00 ± 0.60 at baseline versus 0.02 ± 0.01 after ET-1 stimulation, 1.00 ± 0.10 at baseline versus 0.13 ± 0.02 after ET-1 stimulation, and 1.00 ± 0.17 at baseline versus 0.09 ± 0.04 after ET-1 stimulation for the promoters of *CDH5*, *PDGFB*, *PECAM1*, and *MMP9*, respectively; $P < 0.05$ for all by Mann-Whitney U test). Collectively, these results indicate that ET-1 decreases the DNA binding ability of Fli-1 in HDMECs.

Activation of the c-Abl/PKCδ/Fli-1 pathway in HDMECs by ET-1. We next investigated whether ET-1 activates the c-Abl/PKCδ/Fli-1 pathway in HDMECs. Since ET-1 increases the expression levels of c-Abl and PKCδ in dermal fibroblasts, we first explored its effect on the expression levels of c-Abl and PKCδ in HDMECs. As shown in Figure 2A, as expected, ET-1 stimulation increased the expression levels of c-Abl and PKCδ as early as 15 minutes. Given that the nuclear translocation of

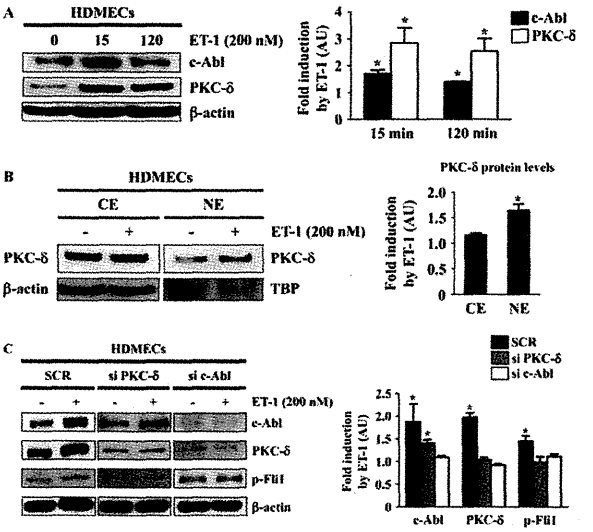

Figure 2. Endothelin 1 (ET-1) activates the c-Abl/protein kinase Cδ (PKCδ)/Fli-1 pathway in human dermal microvascular endothelial cells (HDMECs). **A,** HDMECs were treated with ET-1 (200 n*M*) for the indicated periods of time, and the expression levels of c-Abl and PKCδ were determined by immunoblotting with whole cell lysates (β-actin was used as a control for equal loading). The fold change in the protein levels of c-Abl and PKCδ (quantified by densitometry) was determined. **B,** HDMECs were treated with ET-1 (200 n*M*) or vehicle for 2 hours, and cytoplasmic extracts (CE) and nuclear extracts (NE) were prepared. The expression levels of PKCδ were determined by immunoblotting (β-actin was used as a control for equal loading in the analysis of cytoplasmic extracts, and TATA box binding protein [TBP] was used as a control for equal loading in the analysis of nuclear extracts). The fold change in the protein levels of PKCδ was determined. **C,** HDMECs were treated with scrambled nonsilencing RNA (SCR), small interfering RNA (siRNA) for PKCδ, and siRNA for c-Abl for 48 hours, with or without addition of ET-1 (200 n*M*) for 2 hours. Whole cell lysates were subjected to immunoblotting for c-Abl, PKCδ, and phospho–Fli-1 (β-actin was used as a control for equal loading). The fold change in the protein levels of each molecule (quantified by densitometry) in response to ET-1 as compared to unstimulated controls (set at 1) was determined. Values are the mean ± SEM (n = 3 mice per group). * = $P < 0.05$ versus control cells not treated with ET-1.

PKCδ reflects its activation status, we also evaluated nuclear localization of PKCδ. Consistent with our expectations, ET-1 promoted the nuclear translocation of PKCδ (Figure 2B). To further confirm that c-Abl activation sequentially induces PKCδ activation and Fli-1 phosphorylation, we examined the effect of small interfering RNA (siRNA) against c-Abl or PKCδ on the expression levels of c-Abl and PKCδ and the phosphorylation levels of Fli-1 induced by ET-1. As shown in Figure 2C, c-Abl siRNA inhibited PKCδ induction and Fli-1 phosphorylation, while PKCδ siRNA attenuated Fli-1 phosphorylation, but not c-Abl induction. These results indicate that c-Abl is required for ET-1–dependent PKCδ activation, consistent with sequential activation of the c-Abl/PKCδ/Fli-1 pathway in HDMECs as well as in dermal fibroblasts.

Bosentan suppresses the c-Abl/PKCδ/Fli-1 pathway by inhibiting autocrine endothelin signaling in HDMECs. Since endothelin is an autocrine/paracrine peptide (mainly produced by endothelial cells) that is indispensable in the maintenance of vascular homeostasis in vivo, we next examined the role of autocrine endothelin in the regulation of the DNA binding ability of Fli-1 in HDMECs. To this end, we used a dual endothelin receptor antagonist, bosentan, and investigated its effect on the c-Abl/PKCδ/Fli-1 pathway in HDMECs. Since bosentan at 10, 20, and 40 μM did not affect the viability of HDMECs evaluated by trypan blue exclusion test (data not shown), we used 20 μM of bosentan in the subsequent experiments. As shown in Figures 3A and B, bosentan suppressed the expression of the c-Abl and PKCδ proteins, the phosphorylation levels of Fli-1, and the nuclear localization of PKCδ, while increasing Fli-1 protein levels, in HDMECs. Collectively, these results indicate that the autocrine endothelin pathway regulates the transcriptional activity of Fli-1 in HDMECs.

Four weeks of treatment with bosentan alleviates vascular fragility, but not abnormal vascular structure, in Fli-1 ECKO mice by increasing endothelial Fli-1 expression. In order to investigate the effect of bosentan on the expression levels of Fli-1 in endothelial cells in vivo, bosentan (20 mg/kg) was given intraperitoneally to Fli-1 ECKO mice and WT mice for 4 weeks (this did not affect the viability of bleomycin-treated mice in our previous study [17]), and Fli-1 protein levels were determined by immunohistochemistry analysis. As shown in Figure 4A, Fli-1 was expressed abundantly in dermal microvascular endothelial cells of WT mice treated with saline, while Fli-1 expression levels were highly variable in dermal microvascular endothelial cells of saline-treated Fli-1 ECKO mice due to the variable efficiency of the Cre

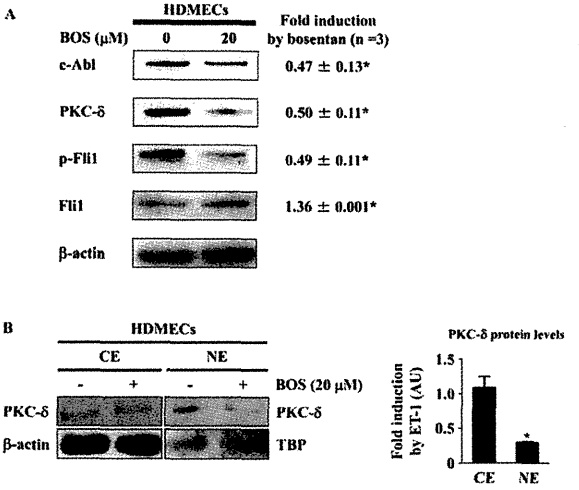

Figure 3. Impact of bosentan (BOS) on the c-Abl/protein kinase Cδ (PKCδ)/Fli-1 pathway in human dermal microvascular endothelial cells (HDMECs). **A,** HDMECs were treated for 48 hours with bosentan (20 μM), and whole cell lysates were subjected to immunoblotting for c-Abl, PKCδ, phospho–Fli-1, and Fli-1 (β-actin was used as a control for equal loading). The fold change in the protein level of each molecule (quantified by densitometry) in response to endothelin 1 (ET-1) as compared to unstimulated controls (set at 1) was determined. **B,** HDMECs were treated with bosentan (20 μM) or vehicle for 48 hours, and cytoplasmic extracts (CE) and nuclear extracts (NE) were prepared (β-actin was used as a control for equal loading in the analysis of cytoplasmic extracts, and TATA box binding protein [TBP] was used as a control for equal loading in the analysis of nuclear extracts). The fold change in the protein level of each molecule in response to ET-1 as compared to unstimulated controls (set at 1) was determined. Values are the mean ± SEM (n = 3 mice per group). * = $P < 0.05$ versus control cells not treated with ET-1.

enzyme in individual endothelial cells (data available upon request from the corresponding author). After treatement with bosentan, the expression levels of Fli-1 protein were substantially increased in endothelial cells of Fli-1 ECKO mice, while the abundant expression of Fli-1 in endothelial cells of WT mice was not altered after the treatment. These results indicate that bosentan increases Fli-1 protein levels in dermal microvascular endothelial cells in vivo.

As previously reported, Fli-1 ECKO mice exhibit the structural and functional abnormalities of SSc vasculopathy, including distortion of arterioles with thickened and occluded vascular walls and increased vascular permeability due to fragile capillaries (16). To investigate the effect of bosentan on vasculopathy of Fli-1 ECKO mice, we first compared vascular permeability by injecting Evans blue dye into mice treated with either bosentan or saline.

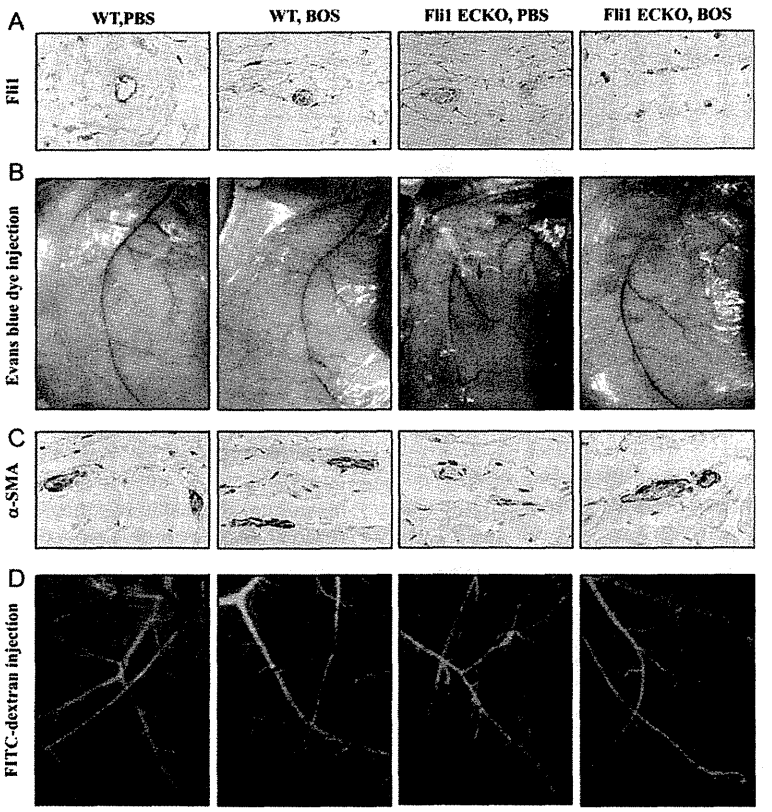

Figure 4. Effect of bosentan (BOS) on vascular abnormalities in endothelial cell–specific Fli-1–knockout (Fli-1 ECKO) mice. **A,** Wild-type (WT) mice and Fli-1 ECKO mice were injected intraperitoneally with bosentan or phosphate buffered saline (PBS) for 4 weeks. Levels of Fli-1 protein in dermal microvascular endothelial cells were evaluated by immunohistochemistry. **B,** Evans blue dye was injected into the tail vein, and the mice were killed after 30 minutes. The leakage of Evans blue dye (**arrows**) was macroscopically evaluated in the skin. **C,** Levels of α-smooth muscle actin (α-SMA) were determined by immunohistochemistry. **D,** Mice were injected with fluorescein isothiocyanate (FITC)–conjugated dextran and killed after 5 minutes. The structure of dermal small vessels was examined by fluorescence microscopy. Results are representative of 5 independent experiments.

As shown in Figure 4B, consistent with results of a previous study (16), extensive vascular leakage was observed in the skin of saline-treated Fli-1 ECKO mice, but not saline-treated WT mice. In contrast, vascular leakage was greatly diminished in Fli-1 ECKO mice that were treated with bosentan for 4 weeks. Since the altered phenotype of pericytes is closely related to vascular fragility of capillaries, leading to increased vascular permeability (16,21), we also investigated expression levels of α-SMA, a marker of pericytes closely interacting with endothelial cells, i.e., vascular stabilization. Consistent with results of a previous study (16), α-SMA expression was markedly decreased in dermal small vessels of Fli-1 ECKO mice treated with saline when compared to dermal blood vessels of saline-treated WT mice (Figure 4C). After 4 weeks of bosentan treatment, α-SMA expression was increased in dermal small vessels of Fli-1 ECKO mice, suggesting that bosentan promotes vascular stabilization in these mice.

We next examined the effect of bosentan on vascular structure, as visualized by FITC-conjugated dextran injection. As shown in Figure 4D, vascular distortion was evident in saline-treated Fli-1 ECKO mice, while vascular structure was well-organized in saline-treated WT mice. After 4 weeks of bosentan treatment, in contrast to the results seen with injection of Evans blue dye, no notable difference was seen in the vascular structure of WT and Fli-1 ECKO mice as compared to saline-treated control mice. Since this technique cannot be used to evaluate microcirculation corresponding to human nailfold capillaries, the effect of bosentan on the morphology of microvasculature in Fli-1 ECKO mice remains unclear.

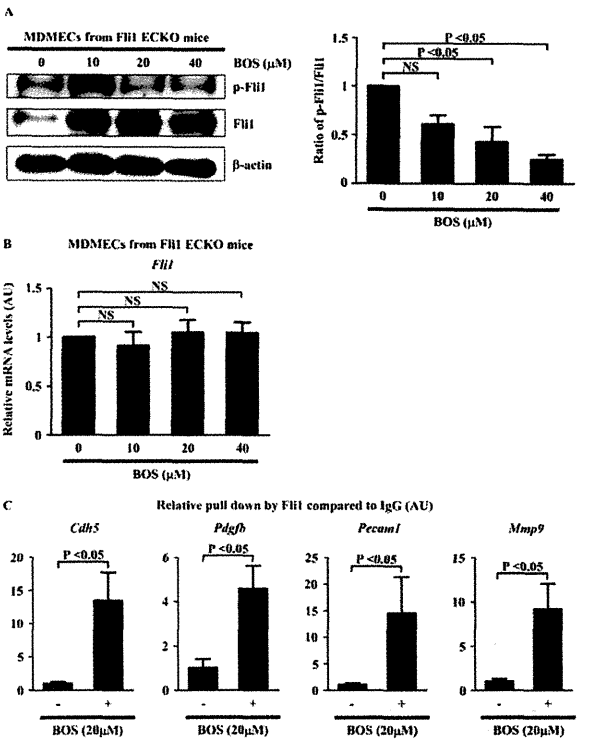

Figure 5. Effect of bosentan (BOS) on dermal microvascular endothelial cells derived from endothelial cell–specific Fli-1–knockout (Fli-1 ECKO) mice. **A,** Mouse dermal microvascular endothelial cells (MDMECs) isolated from Fli-1 ECKO mice were treated for 48 hours with bosentan at the indicated concentrations, and the expression and phosphorylation levels of Fli-1 were determined by immunoblotting with whole cell lysates (β-actin was used as a control for equal loading). The fold change in the ratio of phospho–Fli-1 to total Fli-1 (quantified by densitometry) was determined. **B,** Levels of mRNA for Fli-1 after the same treatment as described in **A** were evaluated by quantitative reverse transcription–polymerase chain reaction (qRT-PCR). **C,** MDEMCs were treated with bosentan (20 μ*M*) or vehicle for 48 hours and analyzed by chromatin immunoprecipitation. Binding of Fli-1 to the target gene promoters (*Cdh5*, *Pdgfb*, *Pecam1*, and *Mmp9*) in response to bosentan as compared to unstimulated controls (set at 1) was quantified by qRT-PCR. Values are the mean ± SEM (n = 3 mice per group in **A** and **B** and 4 mice per group in **C**). NS = not significant.

To further confirm the effect of bosentan on dermal microvascular endothelial cells in Fli-1 ECKO mice, we isolated MDMECs from Fli-1 ECKO mice and treated them with bosentan for 48 hours. As shown in Figures 5A and B, bosentan increased Fli-1 protein levels, with a dose-dependent decrease of the ratio of phospho–Fli-1 to total Fli-1 (the mean ± SEM ratio of phospho–Fli-1 to total Fli-1 compared with baseline was 0.61 ± 0.09, 0.43 ± 0.15, and 0.24 ± 0.05 with 10 μ*M*, 20 μ*M*, and 40 μ*M* of bosentan, respectively; $P = 0.0034$ by one-way ANOVA, $P < 0.05$ for baseline versus 20 or 40 μ*M* of bosentan by Tukey's post hoc test) (Figure 5A), but not Fli-1 mRNA levels (the mean ± SEM relative expression level of Fli-1 mRNA compared with baseline was 0.91 ± 0.14, 1.05 ± 0.13, and 1.05 ± 0.11 with 10 μ*M*, 20 μ*M*, and 40 μ*M* of bosentan, respectively; $P = 0.80$ by one-way ANOVA) (Figure 5B), suggesting that bosentan alters Fli-1 levels by inhibiting its degradation.

The binding of Fli-1 to target gene promoters in MDMECs was also markedly magnified by bosentan (the mean ± SEM relative pulldown by Fli-1 compared to IgG was 1.00 ± 0.24 at baseline versus 13.50 ± 4.22 after bosentan treatment, 1.00 ± 0.40 at baseline versus 4.58 ± 1.04 after bosentan treatment, 1.00 ± 0.33 at baseline versus 14.50 ± 6.84 after bosentan treatment, and 1.00 ± 0.28 at baseline versus 9.19 ± 2.86 after bosentan treatment for the promoters of *Cdh5*, *Pdgfb*, *Pecam1*, and *Mmp9*, respectively; $P < 0.05$ for all by Mann-Whitney U test) (Figure 5C). Collectively, these results indicate that bosentan reverses Fli-1 deficiency–dependent vasculopathy by increasing the transcriptional activity of Fli-1.

DISCUSSION

This study was based on the hypothesis that bosentan augments the transcriptional activity of Fli-1 by increasing its expression and DNA binding ability in endothelial cells. In support of our hypothesis, in HDMECs, ET-1 activated the c-Abl/PKCδ/Fli-1 pathway, leading to a decrease in expression levels and promoter binding ability of Fli-1, and bosentan augmented the transcriptional activity of Fli-1 by increasing its expression and promoter binding ability through the blockade of autocrine endothelin. Given that blockade of the c-Abl/PKCδ/Fli-1 pathway increases the protein levels of Fli-1 by increasing its protein stability while not affecting its mRNA levels (8,9,22), bosentan would theoretically be able to increase levels of Fli-1 protein in endothelial cells of Fli-1 ECKO mice (in which endothelial Fli-1 expression is reduced by 50–80% due to Cre-mediated deletion of the floxed sequences in the *Fli1* gene) (16). Consistent with this hypothesis, in Fli-1 ECKO mice, 4 weeks of treatment with bosentan increased the protein levels of Fli-1 in dermal microvascular endothelial cells and improved vascular leakage by promoting vascular stabilization characterized by α-SMA expression in pericytes. Collectively, these results indicate that the ET-1 signaling pathway targets Fli-1 in endothelial cells, and bosentan reverses some of the vascular defects related to endothelial Fli-1 deficiency in animal models.

SSc vasculopathy is believed to be caused by aberrant vascular remodeling due to impaired angiogenesis and vasculogenesis, the molecular mechanism of which still remains unclear (23,24). In the dermal microvessels of lesional SSc skin, the expression of α-SMA, a marker of pericytes with an angiostatic phenotype, is decreased (16), while the expression of regulator of G protein signaling 5, a marker of pericytes with an angiogenic phenotype, is elevated (25). This phenotypic change of pericytes suggests that SSc dermal microvessels are unstable and fragile with proangiogenic properties, probably reflecting a compensatory response in order to maintain vascular function. Vascular destabilization in SSc is attributable to the down-regulation of molecules relevant to vascular stabilization, such as VE-cadherin, PECAM-1, and PDGFβ, and the up-regulation of the enzyme that degrades vascular basement membrane, MMP-9. Importantly, the altered expression of these molecules is recapitulated in dermal blood vessels of Fli-1 ECKO mice (16).

Furthermore, the expression profile of angiogenesis-related molecules, including cathepsin V, cathepsin B, and CXCL5, in SSc dermal blood vessels is also reproduced in Fli-1 ECKO mice (12,13,18). Considering that Fli-1 ECKO mice are characterized by leaky and fragile capillaries and thickened and occluded arterioles similar to those seen in SSc (16), Fli-1 deficiency may largely contribute to the induction of the SSc vascular phenotype. Epigenetic suppression has previously been implicated in the mechanism causing Fli-1 deficiency in SSc (14), but results of the present study suggest that ET-1 may also be involved in the down-regulation of Fli-1 in SSc dermal microvascular endothelial cells. This notion is consistent with the previous clinical observation that circulating ET-1 levels are elevated in SSc patients with the diffuse cutaneous involvement that usually accompanies extensive microangiopathy and severe vascular complications, such as pulmonary arterial hypertension and scleroderma renal crisis (26–28).

Since Fli-1 is a potential predisposing factor in SSc (29,30), the normalization of Fli-1 expression may partially improve clinical symptoms of this disease. Given that Fli-1 has been shown to be epigenetically suppressed in SSc skin and dermal fibroblasts (14), the use of epigenetic inhibitors to restore Fli-1 levels may be a potential therapeutic strategy for SSc. However, the systemic administration of epigenetic inhibitors raises serious concerns related to the nonspecific activation of unrelated genes. On the other hand, bosentan has a unique property that augments Fli-1 protein levels even in cells with genetically reduced Fli-1 mRNA levels, as has been demonstrated in Fli-1 ECKO mice. Therefore, bosentan is capable of increasing Fli-1 protein levels even though its expression is strongly suppressed by an epigenetic mechanism, suggesting that endothelin receptor blockade has a potential therapeutic impact on SSc vasculopathy beyond the reversal of the pathologic effects of ET. This theory is consistent with prior reported clinical data. For example, 1 year of treatment with bosentan, but not iloprost, increases the number of nailfold capillaries with early and active patterns (i.e., enlarged capillaries, megacapillaries, and hemorrhages) and decreases the number of nailfold capillaries with late patterns (i.e., capillary loss, ramified capillaries, and capillary disorganization) (4). Furthermore, 3 years of combination therapy with bosentan and iloprost increases the number of nailfold capillaries, while iloprost alone results in a significant decrease in the number of nailfold capillaries (5). Importantly, the beneficial effect of bosentan on SSc vasculopathy was only modest and limited in these studies (a reasonable result since Fli-1 deficiency is one of the predisposing factors in this disease).

As shown in the RAPIDS-1 and RAPIDS-2 studies (Randomized Placebo-controlled studies on prevention of Ischemic Digital ulcers in Scleroderma), bosentan prevents the development of new digital ulcers in SSc without having an effect on healing of preexisting digital ulcers (2,3). The presence of ulnar artery occlusion is closely related to new or recurrent onset of digital ulcers in SSc (31). Since ET-1 plays a critical role in the development of proliferative obliterative vasculopathy by inducing fibroproliferative changes in the vessel wall (32,33), bosentan has been believed to elicit a significant preventive effect on digital ulcers by improving peripheral circulation through a potential reverse remodeling effect as well as a potent vasodilatory effect. On the other hand, ET-1 also plays a part in pathologically activated angiogenesis. For instance, bosentan alleviates increased neovascularization and leaky vessels in the cerebrovascular system in an animal model of type 2 diabetes and inhibits tumor vascularization and bone metastasis in an animal model of breast carcinoma cell metastasis (34,35). This is also the case in SSc, since, as noted above, the number of nailfold ramified capillaries (a reflection of activated angiogenesis) has been found to be decreased after 1 year of treatment with bosentan (4).

As a result of its dual, conflicting effects on SSc vasculopathy (the improvement of peripheral circulation and the inhibition of angiogenesis), bosentan would not be expected to have a beneficial impact on preexisting digital ulcers in SSc (2,3). However, as reported by Cutolo et al (5), combination therapy with

bosentan and iloprost, but not iloprost alone, increases the number of nailfold ramified capillaries, suggesting that combination therapy, but neither bosentan nor iloprost alone, promotes angiogenesis. Although combination therapy with bosentan and prostanoids was not allowed in the RAPIDS-1 and RAPIDS-2 studies, combination therapy may promote angiogenesis in SSc, potentially leading to a beneficial effect on digital ulcers, in which the normalization of Fli-1 protein expression in endothelial cells may be involved. To address this issue, further studies are under way in our laboratory. Although the reported clinical effect of bosentan described above is at best marginal, the elucidation of its molecular mechanism provides us with a useful clue for the further development of therapeutic strategies for SSc vasculopathy.

In summary, this is the first report to demonstrate a possible molecular basis for the impact of endothelin receptor blockade on SSc vasculopathy. Normalization of the expression levels of a potential predisposing factor of SSc (the transcription factor Fli-1) strongly indicates that the combination of bosentan with conventional therapies may ameliorate a broad spectrum of pathologic processes in SSc.

AUTHOR CONTRIBUTIONS

All authors were involved in drafting the article or revising it critically for important intellectual content, and all authors approved the final version to be published. Dr. Asano had full access to all of the data in the study and takes responsibility for the integrity of the data and the accuracy of the data analysis.

Study conception and design. Akamata, Asano, Sato.

Acquisition of data. Akamata, Asano, Noda, Takahashi, Ichimura, Toyama, Trojanowska.

Analysis and interpretation of data. Akamata, Asano, Yamashita, Taniguchi, Toyama, Trojanowska, Sato.

REFERENCES

1. Asano Y. Future treatments in systemic sclerosis. J Dermatol 2010;37:54–70.
2. Korn JH, Mayes M, Matucci Cerinic M, Rainisio M, Pope J, Hachulla E, et al, for the RAPIDS-1 Study Group. Digital ulcers in systemic sclerosis: prevention by treatment with bosentan, an oral endothelin receptor antagonist. Arthritis Rheum 2004;50: 3985–93.
3. Matucci-Cerinic M, Denton CP, Furst DE, Mayes MD, Hsu VM, Carpentier P, et al. Bosentan treatment of digital ulcers related to systemic sclerosis: results from the RAPIDS-2 randomised, double-blind, placebo-controlled trial. Ann Rheum Dis 2011;70:32–8.
4. Guiducci S, Bellando Randone S, Bruni C, Carnesecchi G, Maresta A, Iannone F, et al. Bosentan fosters microvascular deremodelling in systemic sclerosis. Clin Rheumatol 2012;31:1723–5.
5. Cutolo M, Zampogna G, Vremis L, Smith V, Pizzorni C, Sulli A. Longterm effects of endothelin receptor antagonism on microvascular damage evaluated by nailfold capillaroscopic analysis in systemic sclerosis. J Rheumatol 2013;40:40–5.
6. Hettema ME, Zhang D, Stienstra Y, Smit AJ, Bootsma H, Kallenberg CG. No effects of bosentan on microvasculature in patients with limited cutaneous systemic sclerosis. Clin Rheumatol 2009;28:825–33.
7. Shah P, Murray AK, Moore TL, Herrick AL. Effects of iloprost on microvascular structure assessed by nailfold videocapillaroscopy: a pilot study. J Rheumatol 2011;38:2079–80.
8. Asano Y, Czuwara J, Trojanowska M. Transforming growth factor-β regulates DNA binding activity of transcription factor Fli1 by p300/CREB-binding protein-associated factor-dependent acetylation. J Biol Chem 2007;282:34672–83.
9. Asano Y, Trojanowska M. Phosphorylation of Fli1 at threonine 312 by protein kinase C δ promotes its interaction with p300/CREB-binding protein-associated factor and subsequent acetylation in response to transforming growth factor β. Mol Cell Biol 2009;29:1882–94.
10. Asano Y, Trojanowska M. Fli1 represses transcription of the human α2(I) collagen gene by recruitment of the HDAC1/p300 complex. PLoS One 2013;8:e74930.
11. Nakerakanti SS, Kapanadze B, Yamasaki M, Markiewicz M, Trojanowska M. Fli1 and Ets1 have distinct roles in connective tissue growth factor/CCN2 gene regulation and induction of the profibrotic gene program. J Biol Chem 2006;281:25259–69.
12. Noda S, Asano Y, Akamata K, Aozasa N, Taniguchi T, Takahashi T, et al. A possible contribution of altered cathepsin B expression to the development of skin sclerosis and vasculopathy in systemic sclerosis. PLoS One 2012;7:e32272.
13. Noda S, Asano Y, Takahashi T, Akamata K, Aozasa N, Taniguchi T, et al. Decreased cathepsin V expression due to Fli1 deficiency contributes to the development of dermal fibrosis and proliferative vasculopathy in systemic sclerosis. Rheumatology (Oxford) 2013;52:790–9.
14. Wang Y, Fan PS, Kahaleh B. Association between enhanced type I collagen expression and epigenetic repression of the FLI1 gene in scleroderma fibroblasts. Arthritis Rheum 2006;54:2271–9.
15. Kubo M, Czuwara-Ladykowska J, Moussa O, Markiewicz M, Smith E, Silver RM, et al. Persistent down-regulation of Fli1, a suppressor of collagen transcription, in fibrotic scleroderma skin. Am J Pathol 2003;163:571–81.
16. Asano Y, Stawski L, Hant F, Highland K, Silver R, Szalai G, et al. Endothelial Fli1 deficiency impairs vascular homeostasis: a role in scleroderma vasculopathy. Am J Pathol 2010;176:1983–98.
17. Akamata K, Asano Y, Aozasa N, Noda S, Taniguchi T, Takahashi T, et al. Bosentan reverses the pro-fibrotic phenotype of systemic sclerosis dermal fibroblasts via increasing DNA binding ability of transcription factor Fli1. Arthritis Res Ther 2014;16:R86.
18. Ichimura Y, Asano Y, Akamata K, Takahashi T, Noda S, Taniguchi T, et al. Fli1 deficiency contributes to the suppression of endothelial CXCL5 expression in systemic sclerosis. Arch Dermatol Res 2014;306:331–8
19. Asano Y, Ihn H, Yamane K, Kubo M, Tamaki K. Increased expression levels of integrin αVβ5 on scleroderma fibroblasts. Am J Pathol 2004;164:1275–92.
20. Ihn H, Tamaki K. Competition analysis of the human α2(I) collagen promoter using synthetic oligonucleotides. J Invest Dermatol 2000;114:1011–6.
21. Von Tell D, Armulik A, Betsholtz C. Pericytes and vascular stability. Exp Cell Res 2006;312:623–9.
22. Bujor AM, Asano Y, Haines P, Lafyatis R, Trojanowska M. The c-Abl tyrosine kinase controls protein kinase Cδ–induced Fli-1 phosphorylation in human dermal fibroblasts. Arthritis Rheum 2011;63:1729–37.
23. Distler JH, Gay S, Distler O. Angiogenesis and vasculogenesis in systemic sclerosis. Rheumatology (Oxford) 2006;45 Suppl 3:iii26–7.
24. Rabquer BJ, Koch AE. Angiogenesis and vasculopathy in systemic sclerosis: evolving concepts. Curr Rheumatol Rep 2012;14:56–63.
25. Fleming JN, Nash RA, McLeod DO, Fiorentino DF, Shulman HM, Connolly MK, et al. Capillary regeneration in scleroderma: stem cell therapy reverses phenotype? PLoS One 2008;3:e1452.

26. Yamane K, Miyauchi T, Suzuki N, Yuhara T, Akama T, Suzuki H, et al. Significance of plasma endothelin-1 levels in patients with systemic sclerosis. J Rheumatol 1992;19:1566–71.
27. Vancheeswaran R, Magoulas T, Efrat G, Wheeler-Jones C, Olsen I, Penny R, et al. Circulating endothelin-1 levels in systemic sclerosis subsets: a marker of fibrosis or vascular dysfunction? J Rheumatol 1994;21:1838–44.
28. Penn H, Quillinan N, Khan K, Chakravarty K, Ong VH, Burns A, et al. Targeting the endothelin axis in scleroderma renal crisis: rationale and feasibility. QJM 2013;106:839–48.
29. Asano Y, Bujor AM, Trojanowska M. The impact of Fli1 deficiency on the pathogenesis of systemic sclerosis. J Dermatol Sci 2010;59:153–62.
30. Mayes MD, Trojanowska M. Genetic factors in systemic sclerosis. Arthritis Res Ther 2007;9 Suppl 2:S5.
31. Frerix M, Stegbauer J, Dragun D, Kreuter A, Weiner SM. Ulnar artery occlusion is predictive of digital ulcers in SSc: a duplex sonography study. Rheumatology (Oxford) 2012;51:735–42.
32. Hasegawa M, Nagai Y, Tamura A, Ishikawa O. Arteriographic evaluation of vascular changes of the extremities in patients with systemic sclerosis. Br J Dermatol 2006;155:1159–64.
33. Ichimura Y, Asano Y, Hatano M, Tamaki Z, Takekoshi T, Kogure A, et al. Significant attenuation of macrovascular involvement by bosentan in a patient with diffuse cutaneous systemic sclerosis with multiple digital ulcers and gangrene. Mod Rheumatol 2011;21:548–52.
34. Abdelsaid M, Kaczmarek J, Coucha M, Ergul A. Dual endothelin receptor antagonism with bosentan reverses established vascular remodeling and dysfunctional angiogenesis in diabetic rats: relevance to glycemic control. Life Sci 2014;118:268–73.
35. Dreau D, Karaa A, Culberson C, Wyan H, McKillop IH, Clemens MG. Bosentan inhibits tumor vascularization and bone metastasis in an immunocompetent skin-fold chamber model of breast carcinoma cell metastasis. Clin Exp Metastasis 2006;23:41–53.

DOI 10.1002/art.39160

Erratum

In the letter by Zeidler published in the April 2015 issue of *Arthritis & Rheumatology* (pages 1138–1139), there were errors in a table heading and in two reference citations. The heading for the fourth column of the table should have read "Treatment effect in arthritis." The last sentence of the third paragraph of text (with the corrected reference citation) should have read "Moreover, peripheral arthritis was present in 36.3% of patients classified as having axial SpA in the original study involved in the development of the ASAS classification criteria for axial SpA (2)." The last sentence of the fifth paragraph of text (with the corrected reference citation) should have read "Moreover, anti-TNF agents effectively reduced the swollen joint count in patients with nonradiographic SpA (Table 1) (1,5,8)."

We regret the errors.

RHEUMATOLOGY

Rheumatology 2015;54:1308–1316
doi:10.1093/rheumatology/keu479
Advance Access publication 23 December 2014

Original article

Increased expression of chemerin in endothelial cells due to Fli1 deficiency may contribute to the development of digital ulcers in systemic sclerosis

Kaname Akamata, Yoshihide Asano, Takashi Taniguchi, Takashi Yamashita, Ryosuke Saigusa, Kouki Nakamura, Shinji Noda, Naohiko Aozasa, Tetsuo Toyama, Takehiro Takahashi, Yohei Ichimura, Hayakazu Sumida, Yayoi Tada, Makoto Sugaya, Takafumi Kadono and Shinichi Sato

Abstract

Objectives. Chemerin is a member of adipocytokines with a chemoattractant effect on plasmacytoid dendritic cells and macrophages and pro-angiogenic properties. We investigated the potential role of chemerin in the development of SSc.

Methods. Chemerin expression was evaluated by immunostaining and/or real-time quantitative RT-PCR in human and murine skin. The mechanisms regulating chemerin expression in dermal fibroblasts and endothelial cells were examined using the gene silencing technique and chromatin immunoprecipitation. Serum chemerin levels were determined by ELISA in 64 SSc patients and 19 healthy subjects.

Results. In SSc lesional skin, chemerin was up-regulated in small blood vessels, while it was down-regulated in fibroblasts surrounded with thickened collagen bundles. The decreased expression of chemerin was significantly reversed by TGF-β1 antisense oligonucleotide in cultured SSc dermal fibroblasts and chemerin expression was markedly decreased in dermal fibroblasts of bleomycin-treated mice. Gene silencing of transcription factor Fli1, which binds to the chemerin promoter, induced chemerin expression in human dermal microvascular endothelial cells and $Fli1^{+/-}$ mice exhibited elevated chemerin expression in dermal blood vessels. Serum chemerin levels inversely correlated with estimated glomerular filtration rate in SSc patients with renal dysfunction. In SSc patients with normal renal function, patients with digital ulcers had higher serum chemerin levels than those without.

Conclusion. Chemerin is down-regulated in SSc dermal fibroblasts by autocrine TGF-β, while it is up-regulated in SSc dermal blood vessels through endothelial Fli1 deficiency. Increased chemerin expression in dermal blood vessels may be associated with the development of digital ulcers in SSc.

Key words: systemic sclerosis, chemerin, transforming growth factor β, Fli1, digital ulcers.

Rheumatology key messages

- Chemerin expression is decreased in SSc dermal fibroblasts by autocrine TGF-β stimulation and Fli1 deficiency.
- Chemerin expression is increased in SSc dermal blood vessels due to endothelial Fli1 deficiency.
- Chemerin may be associated with the development of cutaneous proliferative obliterative vasculopathy in SSc.

Introduction

SSc is a multisystem autoimmune disease of unknown aetiology characterized by vascular injury and fibrosis of the skin and certain internal organs [1, 2]. Recently adipocytokines have attracted much attention in the investigation of various autoimmune diseases as molecules comprising pathological cytokine networks. In SSc,

Department of Dermatology, University of Tokyo Graduate School of Medicine, Tokyo, Japan

Submitted 31 July 2014; revised version accepted 17 November 2014

Correspondence to: Yoshihide Asano, Department of Dermatology, University of Tokyo Graduate School of Medicine, 7-3-1 Hongo, Bunkyo-ku, Tokyo 113-8655, Japan. E-mail:yasano-tky@umin.ac.jp

several adipocytokines, including adiponectin [3, 4], visfatin [5], resistin [6], apelin [7] and retinol-binding protein 4 [8], have been implicated in the development of fibrosis, vasculopathy and immune abnormalities through a variety of biological effects.

Chemerin, a member of the adipocytokines, regulates the differentiation and metabolic function of adipocytes and glucose homeostasis [9]. Chemerin was originally isolated from inflamed biological fluids and has multifactorial effects on various cell types through its receptor ChemR23. This adipocytokine is implicated in chemotaxis of immune cells, including plasmacytoid dendritic cells, macrophages and NK cells [10]. In psoriatic skin lesions, fibroblast-derived chemerin largely contributes to the recruitment of plasmacytoid dendritic cells producing a large amount of IFN-α [11]. Chemerin also serves as a pro-angiogenic factor and plays an important role in tumour invasion and metastasis by promoting angiogenesis [12–14]. In epidermal keratinocytes, chemerin is related to host defence by functioning as an antimicrobial peptide [15]. In inflammatory arthritis, the concentration of chemerin in SF is elevated and chemerin activates synovial fibroblasts and promotes joint inflammation and injury [16, 17]. Thus chemerin is potentially related to three major pathological events in SSc: fibroblast activation, aberrant angiogenesis and immune abnormalities.

This study was undertaken to elucidate the role of chemerin in the development of SSc. To this end we conducted a series of experiments with clinical samples and SSc animal models.

Methods

Ethics statement

The study was conducted according to the Declaration of Helsinki and was approved by the ethical committee of the University of Tokyo Graduate School of Medicine. Written informed consent was obtained from all of the patients and healthy controls.

Immunohistochemistry

Skin samples were obtained from the forearms of five dcSSc patients (<1 year) and five closely matched healthy controls. Murine skin sections were prepared from back skin of wild-type C57BL/6 mice treated with 200 μg of bleomycin (BLM) or PBS every other day for 4 weeks and from the back skin of $Fli1^{+/-}$ mice. Immunohistochemistry was performed with a Vectastain ABC kit (Vector Laboratories, Burlingame, CA, USA) and antibodies against chemerin (Bioss, Beijing, China) and ChemR23 (Acris Antibodies, San Diego, CA, USA).

RNA isolation and real-time quantitative RT-PCR in cultured cells and skin samples

Dermal fibroblasts were prepared from six dcSSc patients with <2 years of skin thickening and from the corresponding areas of six closely matched healthy donors as described previously [18]. These six dcSSc patients and six healthy donors were independent of the patient and donor groups providing skin samples for immunohistochemistry. Human dermal microvascular endothelial cells (HDMECs) were purchased and maintained as described previously [19]. Treatment with TGF-β1 antisense oligonucleotide and sense oligonucleotide in dermal fibroblasts, gene silencing of Fli1 in HDMECs, the generation of a BLM-induced murine SSc model, RNA isolation from those cells and skin tissue and real-time quantitative RT-PCR were carried out as described previously [18–23]. The sequences of primers were as follows: human chemerin forward 5′-TGGAATATTTGTGAGGCTGGA-3′ and reverse 5′-CAGGCATTTCCGTTTCCTC-3′; human Fli1 forward 5′-GGATGGCAAGGAACTGTGTAA-3′ and reverse 5′-GGTTGTATAGGCCAGCAG-3′; human glyceraldehyde-3-phosphate dehydrogenase (GAPDH) forward 5′-ACCCACTCCTCCACCTTTGA-3′ and reverse 5′-CATA CCAGGAAATGAGCTTGACAA-3′; mouse chemerin forward 5′-GGAGTGCACAATCAAACCAA-3′ and reverse 5′-TTTTACCCTTGGGGTCCATT-3′; mouse GAPDH forward 5′-CGTGTTCCTACCCCCAATGT-3′ and reverse 5′-TGTCATCATACTTGGCAGGTTTCT-3′.

Chromatin immunoprecipitation assay

The chromatin immunoprecipitation (ChIP) assay was carried out using the EpiQuik ChIP kit (Epigentek, Farmingdale, NY, USA) as described previously [19]. The putative Fli1 binding site in the chemerin promoter was predicted by Tfsitescan (http://www.ifti.org/Tfsitescan/). The primers were as follows: chemerin/F-620, 5′-GAATG GTCAGGAAAGGCAGA-3′; chemerin/R-402, 5′-AGCGTC CCTGAGACACTCAT-3′.

Patients

Serum samples, frozen at −80°C until assayed, were obtained from 64 SSc patients [61 women, 3 men; median age 59 years (25th–75th percentile 49.75–68); disease duration 6 years (25th–75th percentile 2–13.5)] and 19 healthy individuals [17 women, 2 men; age 57 years (25th–75th percentile 44.5–62.5)]. Patients treated with CSs or other immunosuppressants prior to their first visit were excluded. Patients were grouped by the LeRoy classification system [24]: 30 patients with lcSSc [29 women, 1 man; age 62.5 years (25th–75th percentile 56.5–73); disease duration 6 years (25th–75th percentile 2.5–15.5)] and 34 with dcSSc [32 women, 2 men; age 57 years (25th–75th percentile 47–62); disease duration 4.5 years (25th–75th percentile 1.5–12.75)]. All dcSSc and 25 lcSSc patients fulfilled the 1980 ACR criteria [24]. Five lcSSc patients not meeting these criteria had sclerodactyly and at least two other features, including calcinosis, RP, oesophageal dysmotility and telangiectasia. Twenty-seven of 34 dcSSc patients and 10 of 30 lcSSc patients had interstitial lung disease, which was defined as bibasilar interstitial fibrosis on chest radiographs or alveolitis on high-resolution CT. As for the autoantibody profile, antibodies against topoisomerase I, centromere, RNA polymerase III, U1RNP and SSA antigens were

detected by ELISAs in 22, 23, 2, 5 and 3 SSc patients, respectively.

Measurement of serum chemerin levels

Specific ELISA kits (R&D Systems, Minneapolis, MN, USA) were used to measure serum chemerin levels in 64 SSc patients and 19 healthy individuals. Briefly, polystyrene 96-well plates coated with anti-chemerin antibodies were incubated with 100-fold diluted serum samples for 2 h. The plates were then washed and incubated with horseradish peroxidase-conjugated anti-chemerin antibodies for 1 h. The wells were then washed again and incubated with stabilized tetramethylbenidine and hydrogen peroxide for 30 min. Finally, the reaction was terminated by 2 N sulphuric acid and the absorbance at 450 nm was measured. Serum chemerin levels were calculated using a standard curve.

Statistical analysis

Statistical analysis was carried out with the Mann–Whitney U-test to compare the distributions of two unmatched groups, with a paired *t*-test for the comparison of paired data after confirming the normal distribution, with the Shapiro–Wilk normality test to confirm a normal distribution, with one-way analysis of variance (ANOVA) followed by the Tukey post hoc test for multiple comparison and with Spearman's rank correlation coefficient to evaluate the correlation with clinical data. Statistical significance was defined as a P-value <0.05.

Results

Chemerin expression in SSc and control skin

We initially examined chemerin expression in normal and SSc skin by immunohistochemistry. In normal skin, chemerin was expressed abundantly in epidermal keratinocytes, moderately in dermal fibroblasts and weakly in dermal small blood vessels (Fig. 1A and B). In SSc skin, in contrast, chemerin expression was elevated in dermal small blood vessels compared with normal skin, whereas chemerin was expressed in epidermal keratinocytes to an extent similar to that in normal skin (Fig. 1C). Notably, chemerin was marginally expressed or totally absent in SSc dermal fibroblasts surrounded with thickened collage bundles (Fig. 1D), while chemerin levels were comparable between SSc dermal fibroblasts located in the area without tissue fibrosis and dermal fibroblasts in normal skin. As for perivascular infiltrates, chemerin expression was variable and no consistent trend was seen in normal and SSc skin. Also, there was no remarkable difference in the expression levels of ChemR23, which was detectable in epidermal keratinocytes, dermal fibroblasts, dermal small blood vessels and inflammatory infiltrates between normal and SSc skin (data not shown). Given the pleiotropic effects of chemerin on various cell types, these results suggest the potential contribution of chemerin to the altered phenotype of SSc dermal fibroblasts and endothelial cells.

FIG. 1 Immunohistochemical analysis for chemerin expression in normal and SSc skin sections

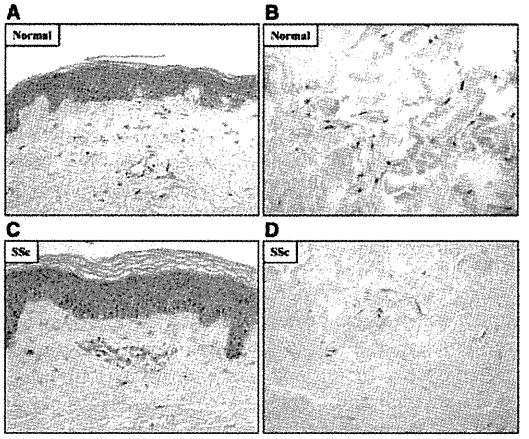

Skin sections from healthy controls (**A** and **B**) and SSc patients (**C** and **D**) were subjected to immunohistochemistry with anti-chemerin antibody. Representative results in the epidermis and endothelial cells (**A** and **C**) and in dermal fibroblasts (**B** and **D**) are shown. Original magnification was 200 × (**A** and **C**) and 400 × (**B** and **D**).

Decreased chemerin expression as a result of autocrine TGF-β and Fli1 deficiency in SSc dermal fibroblasts

To confirm the down-regulation of chemerin in SSc dermal fibroblasts, we looked at chemerin mRNA levels in cultured SSc dermal fibroblasts. As shown in Fig. 2A, chemerin mRNA levels were significantly decreased in SSc dermal fibroblasts compared with normal dermal fibroblasts. To investigate the potential mechanism underlying chemerin suppression in SSc dermal fibroblasts, we focused on TGF-β and transcription factor Fli1 as autocrine TGF-β stimulation and epigenetic suppression of the *Fli1* gene have been shown to contribute to induction of the profibrotic phenotype in SSc dermal fibroblasts [20, 25–27]. As shown in Fig. 2B, in normal dermal fibroblasts, TGF-β1 stimulation significantly suppressed chemerin mRNA levels, which were further decreased by simultaneous silencing of the *Fli1* gene, while gene silencing of Fli1 alone did not affect chemerin expression. Furthermore, Fli1 bound to the chemerin promoter region −620 to −402 bp, which includes the consensus sequence for the Fli1 binding site (GGAT) located at −596 to −593 bp, in normal dermal fibroblasts as confirmed by ChIP assay (Fig. 2C). Moreover, chemerin mRNA levels were significantly higher in SSc dermal fibroblasts treated with TGF-β1 antisense oligonucleotide, which strongly suppresses TGF-β1 expression [20, 21, 25], than in those treated with TGF-β1 sense oligonucleotide, while the levels were comparable between normal fibroblasts treated with TGF-β1 antisense oligonucleotide and those treated with TGF-β1 sense oligonucleotide (Fig. 2D). Collectively these results indicate that chemerin expression is suppressed in SSc

dermal fibroblasts at least partly as a result of autocrine TGF-β and Fli1 deficiency.

Suppressed chemerin expression in the skin of BLM-treated mice

We also evaluated chemerin expression in a BLM-induced murine SSc model, which mimics most of the pathological processes characteristically seen in SSc, including inflammation, autoimmunity and dermal and pulmonary fibrosis. As shown in Fig. 3A, chemerin protein expression was below the detectable level in dermal fibroblasts of BLM-treated mice, while it was abundant in dermal fibroblasts of PBS-treated mice. On the other hand, as for dermal microvascular endothelial cells, chemerin protein expression was marginal in both BLM- and PBS-treated mice (data not shown). Chemerin mRNA levels in the lesional skin were consistently decreased in BLM-treated mice compared with PBS-treated mice (Fig. 3B). These results suggest that chemerin is down-regulated in activated dermal fibroblasts with an SSc-like phenotype.

Fli1 deficiency contributes to the up-regulated expression of chemerin in endothelial cells

We previously demonstrated that gene silencing of Fli1 induces an SSc phenotype in HDMECs at the molecular level, including the decreased expression of vascular endothelial (VE)-cadherin, platelet endothelial cell adhesion molecule 1, PDGF B, $S1P_1$ receptor, cathepsin V and CXCL5 and the increased expression of MMP9 and cathepsin B. More importantly, endothelial cell-specific Fli1 knockout mice reproduce the histological and functional abnormalities of dermal small blood vessels characteristically seen in SSc vasculopathy, such as stenosis of arterioles, dilation of capillaries and increased vascular permeability [19, 28–30]. Thus endothelial Fli1 deficiency is a key molecular feature closely related to the development of SSc vasculopathy. Therefore we investigated the effect of Fli1 small interfering RNA (siRNA) on chemerin expression in HDMECs. As shown in Fig. 4A, Fli1 siRNA treatment resulted in significantly higher induction of chemerin mRNA in HDMECs than scrambled non-silencing RNA. Importantly, Fli1 occupied the chemerin promoter in HDMECs (Fig. 4B) as well as in dermal fibroblasts. To further confirm if endothelial Fli1 deficiency contributes to the induction of chemerin expression in dermal small blood vessels *in vivo*, we carried out immunohistochemistry using skin samples from $Fli1^{+/-}$ mice, which also reproduce the histological and functional abnormalities of dermal small blood vessels similar to SSc vasculopathy to a milder extent than endothelial cell-specific Fli1 knockout mice. Consistent with our idea, chemerin expression in dermal small blood vessels was increased in $Fli1^{+/-}$ mice compared with wild-type mice (Fig. 4C). Collectively these results indicate that Fli1 serves as a potent repressor of the *chemerin* gene in endothelial cells and its haplo-insufficiency results in the up-regulated expression of chemerin in dermal small blood vessels, suggesting that the increased expression of chemerin in dermal small blood vessels of SSc patients may be mediated at least partially by endothelial Fli1 deficiency.

FIG. 2 Chemerin mRNA levels are suppressed as a result of autocrine TGF-β and Fli1 deficiency in SSc dermal fibroblasts

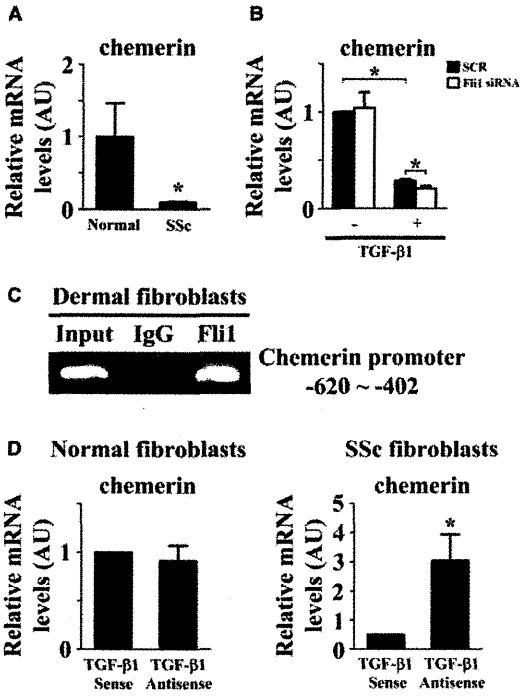

Chemerin mRNA levels were determined by real-time quantitative RT-PCR in confluent quiescent dermal fibroblasts from six SSc patients and six healthy controls (**A**), in normal dermal fibroblasts transfected with scrambled non-silencing small interfering RNA (siRNA) or Fli1 siRNA for 48 h and treated with or without 2 ng/ml of TGF-β1 for the last 24 h (**B**) and in confluent quiescent dermal fibroblasts from four SSc patients and four healthy controls treated with a TGF-β1 antisense oligonucleotide (AS-TGF-β1) or a TGF-β1 sense oligonucleotide (S-TGF-β1) for 48 h (**D**). mRNA levels of the target genes were normalized to mRNA levels of the *GAPDH* gene. Results of controls or relative value compared with controls are expressed as mean (S.E.M.) (**C**) Chromatin was isolated from normal dermal fibroblasts and immunoprecipitated using rabbit anti-Fli1 antibody or rabbit IgG. After isolation of bound DNA, PCR amplification was carried out using chemerin promoter-specific primers. One representative of three independent experiments is shown. Statistical analysis was carried out with the Mann-Whitney *U*-test (**A**) or a paired *t*-test after confirming normal distribution (**B** and **D**). $^*P < 0.05$.

Serum chemerin levels in SSc

As described above, chemerin may play a part in the development of SSc, especially in fibrosis and vasculopathy. To further explore this hypothesis, we evaluated the clinical correlation of serum chemerin levels in SSc patients. Since serum chemerin levels are significantly

FIG. 3 Chemerin expression is decreased in dermal fibroblasts of bleomycin-treated mice

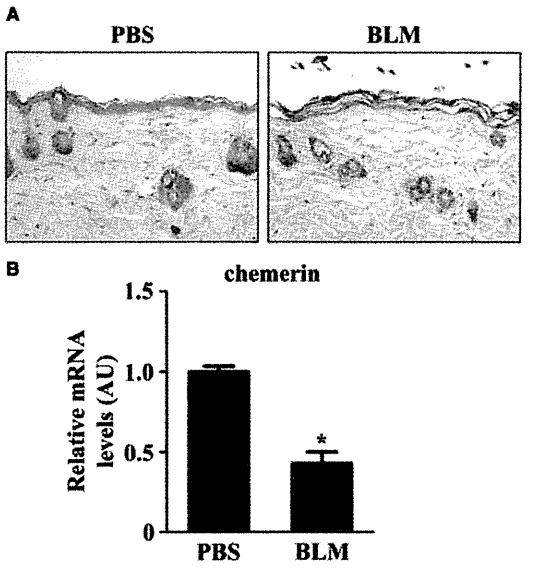

C57BL/6 mice were treated with bleomycin (200 μg) or PBS every other day for 4 weeks. Chemerin expression was evaluated at protein levels by immunohistochemistry (**A**) and at mRNA levels by real-time quantitative RT-PCR (**B**). Results of controls or relative value compared with controls are expressed as mean (S.E.M.) Statistical analysis was carried out with the Mann-Whitney *U*-test. $^*P < 0.05$.

FIG. 4 Chemerin expression is increased in endothelial cells *in vitro* and *in vivo* due to Fli1 deficiency

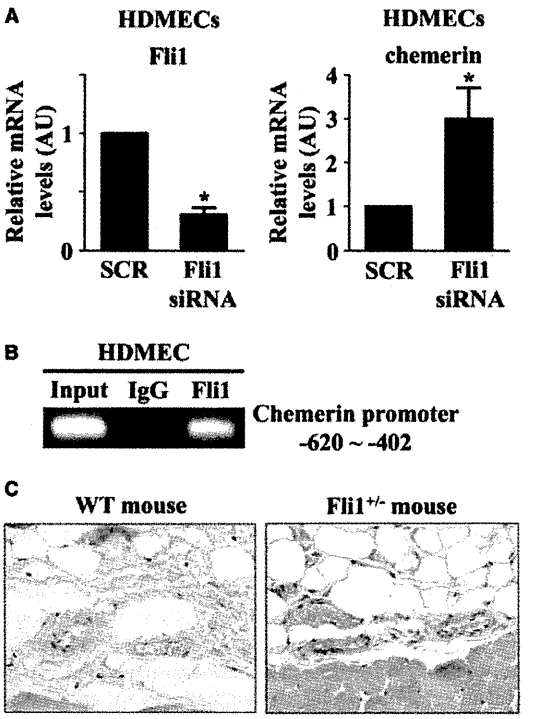

(**A**) HDMECs were transfected with Fli1 small interfering RNA (siRNA) or scrambled non-silencing siRNA (SCR) and mRNA levels of the *Fli1* and *chemerin* genes were determined by real-time quantitative RT-PCR. Results of controls or relative value compared with controls are expressed as mean (S.E.M.) of three independent experiments. Statistical analysis was carried out with a paired *t*-test after confirming normal distribution. $^*P < 0.05$. (**B**) Chromatin was isolated from HDMECs and immunoprecipitated using rabbit anti-Fli1 antibody or rabbit IgG. After isolation of bound DNA, PCR amplification was carried out using chemerin promoter-specific primers. One representative of three independent experiments is shown. (**C**) Immunodetection of chemerin proteins in the skin sections of 3-month-old wild-type and $Fli1^{+/-}$ mice (original magnification 400×). Representative results in five wild-type mice and five $Fli1^{+/-}$ mice are shown.

elevated in patients with chronic kidney disease as compared with closely matched control subjects [31, 32], we classified SSc patients into two groups according to estimated glomerular filtration rate (eGFR), which was calculated from routine creatinine measurements using the Modification of Diet in Renal Disease equation [33], and compared serum chemerin levels. As expected, serum chemerin levels were significantly elevated in SSc patients with an eGFR <60 min/ml/1.73 m^2 as compared with those with an eGFR ⩾60 min/ml/1.73 m^2 [287.5 ng/ml (25th–75th percentile 249.5–367.7) versus 236.4 ng/ml (25th–75th percentile 181.4–289.7), $P < 0.05$]. Importantly, serum chemerin levels inversely correlated with eGFR in SSc patients with eGFR <60 min/ml/1.73 m^2 ($R = -0.90$, $P < 0.0001$; Fig. 5A), while not in SSc patients with eGFR ⩾60 min/ml/1.73 m^2 ($R = -0.11$, $P = 0.44$; Fig. 5B). Collectively, renal function affects serum chemerin levels in SSc patients with eGFR <60 min/ml/1.73 m^2. Therefore we excluded 12 SSc patients with eGFR <60 ml/min/1.73 m^2 (4 dcSSc and 8 lcSSc patients) in the following analyses.

Serum chemerin levels in SSc patients with normal renal function were comparable to those in healthy individuals [236.4 ng/ml (25th–75th percentile 181.4–289.7) *vs* 217.6 ng/ml (25th–75th percentile 196.2–261.7)]. Furthermore, there was no significant difference in serum chemerin levels among dcSSc patients [224.7 ng/ml (25th–75th percentile 175.2–283.3)], lcSSc patients [259.5 ng/ml (25th–75th percentile 197.7–294.6)] and healthy controls (Fig. 5C). However, there were two dcSSc patients with very low serum chemerin levels, suggesting that down-regulation of chemerin may be associated with some aspect of the disease process in dcSSc.

Correlation of serum chemerin levels with disease duration in dcSSc

We next focused on the parameters reflecting dermal and pulmonary fibrotic response, including modified Rodnan

FIG. 5 Serum chemerin levels in SSc patients

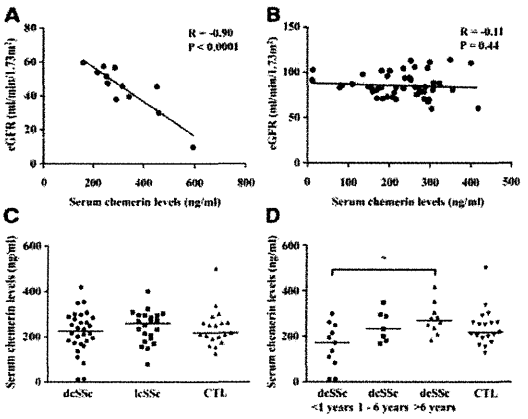

Serum chemerin levels were determined by a specific ELISA in SSc patients and healthy controls. A significant inverse correlation was found between serum chemerin levels and eGFR in SSc patients with renal dysfunction (**A**), while there was no correlation in SSc patients with normal renal function (**B**). The solid line represents the regression line. Statistical analysis was carried out by Spearman's rank correlation test. (**C**) Serum chemerin levels were comparable between dcSSc and lcSSc patients with normal renal function and control subjects (CTL). Horizontal bars indicate the median value in each group. (**D**) The dcSSc patients were divided into three subgroups: those with disease duration <1 year, those with disease duration 1-6 years and those with disease duration >6 years. Disease onset was defined as the first clinical event of SSc other than RP. Disease duration was defined as the interval between onset and time of blood sampling. Horizontal bars indicate the median value in each group. Statistical analysis was conducted with one-way analysis of variance followed by the Tukey post hoc test. $^*P < 0.05$.

total skin thickness score, percentage vital capacity (%VC) and percentage diffusing capacity for carbon monoxide (%DLCO), because dcSSc is characterized by extensive fibrosis especially in skin and lung. Notably, a significant positive correlation was found between serum chemerin levels and modified Rodnan total skin thickness score in dcSSc ($r = 0.43$, $P = 0.021$), while there was no significant correlation of serum chemerin levels with %VC ($r = -0.09$, $P = 0.55$) or %DLCO ($r = -0.17$, $P = 0.51$). These results suggest that serum chemerin levels reflect the severity of skin sclerosis in dcSSc. Alternatively, the reduction of serum chemerin levels may largely contribute to the initiation of fibrosis in the early stage of dcSSc, but not afterwards. Taking into account that serum chemerin levels were comparable between dcSSc patients and healthy controls and that a couple of dcSSc patients had markedly low serum chemerin levels, the latter is plausible. Consistently, serum chemerin levels correlated positively with disease duration in dcSSc ($r = 0.46$, $P = 0.016$). Further supporting this notion, when we classified dcSSc patients into three subgroups according to disease duration as described previously [5, 29, 30]—early dcSSc (disease duration <1 year), midstage dcSSc (disease duration 1-6 years) and late-stage dcSSc (disease duration >6 years)—serum chemerin levels were significantly decreased in early dcSSc compared with late-stage dcSSc (Fig. 5D). Collectively, down-regulation of chemerin may play some role in the developmental process of skin sclerosis in early dcSSc.

Elevated serum chemerin levels in SSc patients with digital ulcers

Since chemerin expression was increased in dermal small blood vessels of SSc patients, we further examined the correlation of serum chemerin levels with vascular symptoms (Table 1). As for cutaneous vascular symptoms, there was a trend towards an increase in serum chemerin levels in SSc patients with RP as compared with those without, while the presence of nail fold bleeding and pitting scars did not affect serum chemerin levels. On the other hand, with organ involvement associated with proliferative obliterative vasculopathy, serum chemerin levels were significantly elevated in SSc patients with digital ulcers as compared with those without, whereas the presence of elevated right ventricular systolic pressure (RVSP) did not affect serum chemerin levels. These results suggest that the increased expression of chemerin in dermal small blood vessels is associated with the development of digital ulcers in SSc patients. Supporting these results of clinical analysis, two dcSSc patients with quite low serum chemerin levels (11.5 and 12.9 ng/ml) were characterized by early disease (disease duration <1 year) without digital ulcers.

Discussion

Our initial findings that chemerin expression is altered in dermal fibroblasts and dermal small blood vessels, but not in inflammatory cells, in SSc skin suggest potential roles of this cytokine in fibrosis and vasculopathy of this disease. To further assess this hypothesis, we evaluated the clinical correlation of serum chemerin levels in SSc patients with normal renal function since renal dysfunction associated with SSc strongly affects serum chemerin levels as well as other pathological conditions with renal dysfunction. Of note, serum chemerin levels were significantly decreased in early dcSSc compared with late-stage dcSSc, which is consistent with the decreased chemerin expression in dermal fibroblasts as a result of autocrine TGF-β in early dcSSc. In contrast, serum chemerin levels were significantly elevated in SSc patients with digital ulcers. There was also a trend towards elevation of serum chemerin levels in SSc patients with RP. Closely related to these clinical data, chemerin was up-regulated in SSc dermal small blood vessels. Viewed altogether, altered expression of chemerin in dermal fibroblasts and dermal small blood vessels may contribute to the development of dermal fibrosis and cutaneous vasculopathy in SSc patients.